# Degradation of Waste Activated Sludge by Combination of Photocatalysis and Anaerobic Digestion

October 2013

Chunguang LIU

# Degradation of Waste Activated Sludge by Combination of Photocatalysis and Anaerobic Digestion

A Dissertation Submitted to

The Graduate School of Life and Environmental Sciences,

the University of Tsukuba

in Partial Fulfillment of the Requirements

for the Degree of Doctor of Philosophy in Environmental Studies

(Doctoral Program in Sustainable Environmental Studies)

**Chunguang LIU**

# Abstract

With population growth and economic development, large amounts of wastewater plants have been built up, resulting in mass production of waste activated sludge (WAS) in the wastewater treatment processes. According to Japan Sewage Works Association, in Japan, about 1.63 Mt sewage sludge was produced in 1994 and increased to 2.17 Mt (dry basis) in 2004 and was estimated to continuously increase in the future. Generally, the WAS is viewed as a kind of typical pollution sources, such as pathogenic microorganisms, eutrophication in water and soil caused by nitrogen, phosphorus and heavy metals pollution. Therefore, with the introduction of stringent regulations and concerns of environmental production, the treatment and disposal of WAS has become one of the most important and complex problems.

Anaerobic digestion can be used to degrade WAS and simultaneously produce biogas, but the relatively long retention time and additional heating limits its wide application. The combination of anaerobic digestion and pretreatment, such as thermal, ultrasonic and microwave, could reduce the retention time and increase the degradation of WAS to some extent but need more energy. $TiO_2$-based solar photocatalysis can be a good alternative to degrade WAS, deactivate pathogenic microorganisms and produce hydrogen with a relatively short retention time at much less energy consumption. Therefore, the aim of this study is to combine photocatalysis with anaerobic digestion to degrade WAS and to produce gas energy simultaneously.

i

Firstly, a catalyst-suspended photocatalytic reactor (sloping trough circulating bed photocatalytic reactor - STCBPR) was developed to pretreat WAS which was used as substrate to produce hydrogen via anaerobic digestion. The effect of the photocatalytic reactor on WAS degradation and the enhancement of photocatalysis on biohydrogen production were mainly investigated. Results showed that the STCBPR was effective in degrading WAS, with nearly 45% of COD removal and 47% of VS reduction under 7.5-fold WAS dilution after reaction for 8 h. In addition, photocatalytic pretreatment could increase the SCOD and $NH_4^+$-N concentrations of the WAS. Moreover, photocatalysis pretreated WAS as substrate produced the maximum hydrogen (53.2 ml-$H_2$/l-sludge for 35 d at 35 ℃) via anaerobic digestion, while the maximum hydrogen production from raw WAS was only 3.1 ml-$H_2$/l-sludge.

Secondly, a catalyst-supported photocatalytic reactor was developed to overcome the problems of catalyst separation and increase of WAS volume caused by direct addition of photocatalyst. To meet the objectives, an efficient photocatalyst was synthesized by doping Ag on $TiO_2$, with its photocatalytic activity (99.5% of methyl orange removal) significantly higher than $TiO_2$ (30.6% of methyl orange removal). Then, a newly-developed solar fluidized tubular photocatalytic reactor (SFTPR) with AgX/$TiO_2$-coated glass tubes was developed to degrade WAS. By using this reactor, 69.1% COD removal and 7866.7 μmol-$H_2$/L-sludge were achieved after solar photocatalysis for 72 h, which was 50% and 350% higher than in SFTPR with $TiO_2$ as

photocatalyst.

Finally, according to the results of photocatalytic degradation of WAS and technology for $AgX/TiO_2$-coating on glass tubes, a photocatalysis anaerobic fermenter was developed with one photocatalytic unit and one anaerobic digestion unit included. The degradation of WAS and methane production via anaerobic digestion at 35ºC with intermittent photocatalytic pretreatment (4 h/day) were investigated. The photocatalysis anaerobic fermenter exhibited the best performance that 60.5% of COD removal and 1266.7 ml-$CH_4$/L-sludge production were obtained in the photocatalytic anaerobic fermenter. While, only 43.5% of COD removal and 932.2 ml-$CH_4$/L-sludge production were obtained in the control fermenter. Moreover, the photocatalytic anaerobic fermenter is easy to operate and maintain, and it can provide a useful reference for the practical application of photocatalysis on WAS treatment.

The obtained results from this research are important and can build up the database for the combined technology (photocatalysis and anaerobic digestion) to be successfully applied in practice.

# Contents

# Chapter 1 Introduction

## 1.1. Sludge production and its environmental issues

With population growth and economic development, a large number of wastewater plants have been built up, resulting in mass production of waste activated sludge (WAS) in wastewater treatment processes. The annual amount of WAS, about 74 million tones on wet basis [1] and 2 million tones on dry basis [2] in Japan, was estimated to continuously increase in the future.

Generally, the WAS is viewed as a kind of typical pollution sources due to its constituents such as pathogenic microorganisms, nitrogen and phosphorus, polymer substances and heavy metals [3], which result in water and soil pollution or eutrophication if being inadequately treated. On the other hand, sludge contains a lot of organics which can be used to produce energy or fertilizer by some technologies. Therefore, with the introduction of stringent regulations and concerns of environmental production, the treatment and disposal of WAS has become one of the most important and complex problems [4].

## 1.2. Sludge treatment and major problems

Sludge treatment refers to sludge reduction, stabilization and disposal. For the sludge reduction (most effectively by dewatering), all kinds of methods can be used, including physical (ultrasonic [5], microwave [6], vacuum filtration, filter press [7]

and centrifuge), chemical (thermal [8], acidic [9] and alkaline [10]) and biological (composing, aerobic [11] and anaerobic digestion [12]) methods. For the stabilization, composing, and aerobic [11] or anaerobic digestion [12] are commonly used. For the disposal of sludge, incineration and landfill are the common methods for sludge treatment.

However, there are some problems for these methods to treat sludge, in consideration of land application, environmental protection, and energy consumption. Physical methods consume much energy and need post-treatment [13]. Chemical methods consume many chemicals and possibly cause secondly environmental pollution [14]. Landfilling is becoming increasingly more difficult to implement because of rapidly shrinking landfill space, public opposition to opening new landfill sites, leachate related issues and, above all, poor economics. In many cases the costs of opening a new landfill is prohibitive simply due to legal restrictions [15]. Composting involves the decomposition of organic materials, and composted sludge can be used as a soil conditioner in agriculture and returns carbon, nitrogen, phosphorus and essential elements back to the soil. However, pathogens and heavy metals can limit the reuse of composted sludge. The most serious environmental concerns related to the incineration of sewage sludge are that it produces significant amounts of dioxin, furan and fly ash. The fly ash contains toxic metals such as lead, cadmium, copper and zinc, as well as dioxins and furans [3]. Anaerobic digestion is an alternative way to treat sludge, because it can dispose sludge with stabilization,

volume reduction, innocent treatment and resource recovery at the same time.

**1.3. Anaerobic digestion**

Anaerobic digestion is a series of processes in which microorganisms break down biodegradable material in the absence of oxygen. Anaerobic digestion with the advantages of low nutrient requirements, high waste removal rate and high efficiency of methane or hydrogen production has been widely used as an attractive waste treatment practice [16]. According to its gaseous products, anaerobic digestion can be classified into hydrogen and methane anaerobic digestion. In contrast to aerobic waste treatment process, it is environmental friendly, low energy consumption and low-cost [17]. In addition, produced methane or hydrogen can be used as clean energy to replace fossil fuel or petroleum.

1.3.1. Theory of anaerobic digestion for hydrogen production

Owing to finite resources and emission of pollutants, hydrogen is a promising alternative to fossil fuels. Hydrogen is a clean energy that produces water instead of greenhouse gases when combusted. Furthermore, hydrogen has a high-energy yield (142.35 kJ/g) that is about 2.75 times that of hydrocarbon fuels. Hydrogen production from biomass is also considered as an alternative energy source in a decentralized power generation scenario [18]. When coupled with the treatment of waste, this process can result in the reduction of pollution from the uncontrolled degradation of

3

waste and the generation of a clean alternative fuel. Anaerobic digestion for hydrogen production process can be summarized as the three path ways [19], shown in Fig.1.1. The first one is that pyruvate is decarboxylated to produce hydrogen. During this process, pyruvate is decarboxylated by pyruvate dehydrogenase and electrons are transferred to the reduction state of ferredoxin (Fdred), and then are re-oxidized into the oxidation state of the ferredoxin (Fdox) by hydrogenase and generate molecular hydrogen. The second is that formic acid is cleaved to produce hydrogen, which is generated by the decarboxylation of acetone and combination of $CO_2$ and $H^+$ under anaerobic condition. The third is that coenzyme (NADH or $NAD^+$) adjust the redox balance for hydrogen production.

1.3.2. Theory of anaerobic digestion for methane production

Methane anaerobic digestion is a biological process in which all kinds of organic matters are degraded and simultaneously produce methane and carbon dioxide under anaerobic conditions. The overall digestion process can be divided into four steps: hydrolysis, acidification, acetogenesis, and methanogenesis [20], as shown in Fig. 1.2. The microorganism community and end products are different in the four steps of anaerobic digestion process of complex substrates, such as waste activated sludge. Hydrolysis is a relatively slow but essential process for the whole anaerobic digestion process. Generally, it limits the rate of the overall anaerobic digestion process due to the presence of refractory organics. In this step, hydrolytic bacteria hydrolyze and

convert the organic compounds into volatile fatty acids with the simultaneous production of hydrogen and carbon dioxide. In the second step (acidogenesis or acidification) various organic acids are produced and the organic acids are converted to acetic acid by the acidogenic and acetogenic bacteria, respectively. In the acetogenesis-step, hydrogen is produced and all kinds of acidification products are converted into acetic acids and carbon dioxide by acetogenic bacteria. In the fourth step, organic material is removed and the acetic acid produced in the third step are converted into $CO_2$ and $CH_4$, which are desorbed from the liquid phase. It is important to note that the pathway of anaerobic digestion process can be controlled to produce hydrogen or methane by changing fermentation conditions, such as substrate, pH, temperature, hydraulic retention time (HRT), and so on.

### 1.3.3. Anaerobic digestion of waste activated sludge

Waste activated sludge (WAS) refers to a kind of surplus activated sludge which is produced in sewage treatment works during the aeration treatment of sewage effluent. It is a kind of complex heterogeneous mixture consisting of microorganisms, colloids, organic polymers and inorganic pollutants [21, 22]. Anaerobic digestion as a sustainable technology to treat waste, such as wastewater and WAS, is accepted for reducing the volume of waste and simultaneously producing energy (hydrogen or methane) [12, 20]. Generally, hydrolysis is the first stage of anaerobic digestion process [23], and it is recognized to be the rate-limiting step in anaerobic digestion

5

process, especially for the hydrolysis of WAS [24], due to its complex composition and containing a lot of refractory materials. On the other hand, hydrolysis is also the essential stage and supply nutritional ingredients for acidogenesis and methanogenesis [25]. Therefore, it is necessary to pretreat the WAS to improve its hydrolysis and further to enhance the biogas production.

## 1.4. Pretreatment methods for the enhancement of WAS biodegradability

In order to improve the degradation of WAS and increase methane yield from WAS via anaerobic digestion, most studies focused on the pretreatment of WAS to accelerate the hydrolysis of WAS. These pretreatments can be mainly classified into three kinds: physical (e.g. as thermal, ultrasonic and microwave) [24, 26, 27], chemical (e.g. as acidic and alkaline) [9, 28] and the combination of physical and chemical methods [26, 29, 30]. Although these pretreatments could improve the degradation of WAS and methane production, some problems still present. Acidic and alkaline pretreatment without heating have less improvement effect on hydrogen production and might cause secondary pollution to the environment due to chemicals addition. Microwave and heating can efficiently enhance the hydrogen production but consume large amounts of energy at the same time. Guo et al. [31] noted that ultrasonic pretreatment would inhibit the hydrogen production due to the production of some inhibitors and extraction of heavy metal ions during pretreatment processes. Wang et al. [32] reported that enzyme pretreatment was an expensive method and had some problems relating with adsorption and desorption from substrate surfaces. Furthermore, WAS could not been hydrolyzed adequately for only initial pretreatment,

along with the consumption of soluble organics in anaerobic digestion process, further pretreatment is necessary to solubilize the refractory organics. However, until now almost no one reported on the intermittent pretreatment during anaerobic methane production process [33].

## 1.5. TiO$_2$ photocatalysis

Titania-based heterogeneous photocatalytic oxidation has received more attention for many years as an alternative method for the purification of wastewater [34]. It has been proved to be an effective technology for removal of refractory organic pollutants in wastewater, owing to its potential application in photoelectron-chemical solar-energy conversion with a high efficiency, photochemical stability, non-toxicity and low cost [35].

### 1.5.1. Theories of photocatalytic degradation and water splitting

The basic photophysical and photochemical principles have been interpreted in many literatures [36, 37]. The mechanisms were shown in Fig. 1.3. Photocatalytic reaction is initiated when a photo-excited electron ($e^-$) is promoted from the valence band (VB) of TiO$_2$ to the conduction band (CB) as the absorbed photo-energy (hv) equals or exceeds the band gap of the TiO$_2$ leaving behind a hole ($h^+$) in the valence band. Thus, electron and hole pair ($e^-/h^+$) is generated simultaneously. The following chain reactions have been widely postulated [34, 38].

Photoexcitation: $TiO_2 + hv \rightarrow e^- + h^+$ (1-1)

7

Recombination: $e^- + h^+ \rightarrow h\nu$ $\qquad$ (1-2)

Formation of superoxide radical: $O_2 + e^- \rightarrow O_2^{\bullet-}$ $\qquad$ (1-3)

Formation of hydroxyl radicals: $OH^- + h^+ \rightarrow \bullet OH$ $\qquad$ (1-4)

Formation of $Ti^{3+}$: $Ti^{4+} + e^- \rightarrow Ti^{3+}$ $\qquad$ (1-5)

Formation of Titanol radicals: $Ti\text{-}OH + h^+ \rightarrow Titanol$ $\qquad$ (1-6)
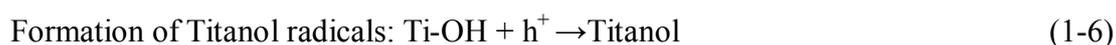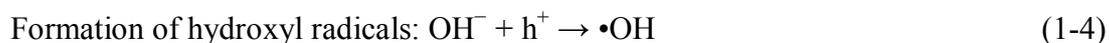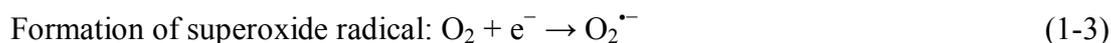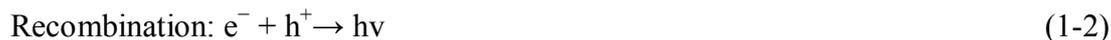
For the photocatalytic water splitting, the redox properties of a photoexcited $TiO_2$ depend predominantly on the energetic positions of the highest energy state of the VB and the lowest energy state of the CB. It is evident from reactions (1-7) and (1-8) that the quasi/Fermi level of electrons in the CB must be > 0 eV to catalyze reduction of water to hydrogen, and similarly the quasi/Fermi level of holes in the VB must be < -1.23 eV to oxidize water in the relatively unfavorable four-hole process [39]:

Reduction of Water: $2H^+ + 2e^- \rightarrow H_2$ ($E^o_{Red}$ = 0 eV) $\qquad$ (1-7)

Oxidation of water: $2H_2O + 4h^+ \rightarrow O_2 + 4H^+$ ($E^o_{Ox}$ = − 1.23 eV) $\qquad$ (1-8)
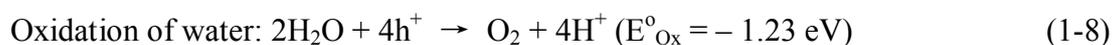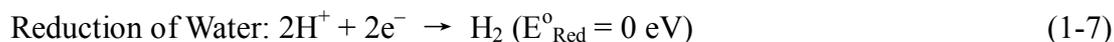
1.5.2. Comparison of $TiO_2$ utilization and photocatalytic reactors

$TiO_2$ photocatalyst can be used either as suspended $TiO_2$ particles or as immobilized on a substrate. Most experiments utilized suspended $TiO_2$ particles in wastewater and leachate treatment, which has higher photocatalytic efficiency but increase the dosage of photocatalyst and the post-treatment cost for the separation of catalyst [40]. The development of photocatalytic membrane reactors solves the drawbacks to some extent. On the other hand, immobilized catalyst do not need

post-treatment for the separation of catalyst but have relatively lower photocatalytic efficiency [41]. Despite aforementioned drawbacks, more immobilized photocatalysts and immobilization techniques are still investigated to enhance photocatalytic activity to treat wastewater and waste.

Photocatalytic reactors for wastewater treatment can generally be classified into two main configurations, depending on the exsiting state of the photocatalysts in the reactor: (i) suspended-type with photocatalyst particles mixed with contaminants in the reactors and (ii) supported-type with photocatalyst immobilized onto inert carrier in the reactor [38]. Based on the two main types, various reactors have been used for the photocatalytic water treatment, including annular photocatalytic reactor [42], common flat photocatalytic reactor [43], film type photocatalytic reactor [44, 45], fluidized bed photocatalytic reactor [46] and optical fiber photocatalytic reactor [47].

The main differences of the two configurations lie in the followings. Boyjoo et al. [48] addressed that the most important factors in configuring a photocatalytic reactor were the total irradiated surface area of catalyst per unit volume and light distribution within the reactor. Catalyst-suspended photocatalytic reactor usually performs a high total surface area of photocatalyst per unit volume. This type of reactor needs to be specifically designed to ensure the maximal illuminated reactor volume with minimal pressure requirement for good catalyst mixing and dispersion. Until recently, the catalyst-suspended photocatalytic reactor was still the preferred configuration owing to its high total surface area of photocatalyst per unit volume and ease of

9

photocatalysts reactivation. The photocatalyst particles can be separated by settling tanks or external cross-flow filtration system to enable continuous operation of the slurry reactor. A technically promising solution for solving the downstream separation of photocatalyst particles after treatment is via the application of hybrid photocatalysis membrane process [49].

Catalyst-supported photocatalytic reactor is often associated with mass transfer limitation over the immobilized layer of photocatalysts. For the photocatalytic treatment of WAS, catalyst-supported photocatalytic reactors would be a better choice, photocatalytic reactions conducting on the surface of photocatalyst. Moreover, its relatively low photocatalytic efficiency could be remedied by a more efficient photocatalyst and higher light intensity.

1.5.3. Factors influencing TiO$_2$ photocatalysis

After the integration of the photocatalyst into a photocatalytic reactor, the oxidation rate and efficiency of the photocatalytic system are highly dependent on a number of the operation parameters [38], including nature, concentration and pH of the substrate, nature and dosage of the photocatalyst, light intensity, photocatalytic reactor [35].

(1) Nature, concentration and pH of the substrate

During photocatalytic oxidation, the concentration of organic substrate over time is dependent on photocatalysis efficiency [50]. At high-substrate concentrations, however, the photocatalysis efficiency declines and the TiO$_2$ surface becomes

10

saturated leading to catalyst deactivation. Moreover, the light transmission of the substrate and content of refractory organics in substrate also influences the photocatalysis efficiency. Low light transmission and high content of refractory organics decrease the photocatalysis efficiency [51].

The substrate pH is another important parameter in photocatalytic reactions taking place on particulate surfaces, since it dictates the surface charge properties of the photocatalyst and size of aggregates it forms [38]. Under acidic or alkaline condition the surface of $TiO_2$ can be protonated or deprotonated respectively according to the following reactions:

$$TiOH + H^+ \rightarrow TiOH_2^+ \tag{1-9}$$

$$TiOH + OH^- \rightarrow TiO^- + H_2O \tag{1-10}$$

Thus, that $TiO_2$ surface will remain positively charged in acidic medium and negatively charged in alkaline medium. $TiO_2$ is reported to have higher oxidizing activity at lower pH but excess $H^+$ (at very low pH) can decrease the reaction rate [52]. Moreover, the addition of HCl to obtain excess $H^+$ leads to increase of cost and second pollution. Therefore, it is a better choice to treat the waste at the original pH value.

(2) Nature and content of the photocatalyst

There is a direct correlation between organic pollutant and surface coverage of $TiO_2$ photocatalyst, since photocatalytic reaction takes place only in the adsorbed phase of the semiconductor particle. The important parameters that influence the performance

11

of photocatalyst in photocatalytic oxidation are particle size and agglomerate size, physical properties, activity, stability and absorption spectra of the photocatalyst [53].

$TiO_2$ can be synthesized by different methods to arrive at a photocatalyst exhibiting desirable physical properties, activity and stability for photocatalytic application [54]. Evidently, there is a clear connection between the surface properties, the rational development of improved synthesis routes and the possible usefulness of the material prepared in application [55]. On the other hand, the rate of photocatalytic reaction is strongly influenced by concentration of the photocatalyst. Heterogeneous photocatalytic reactions are known to show proportional increase in photodegradation with catalyst loading. Generally, in any given photocatalytic application, the optimum catalyst concentration must be determined, in order to avoid excess catalyst and ensure total absorption of efficient photons [38]. This is because an unfavorable light scattering and reduction of light penetration into the solution has been observed if with excess photocatalyst loading [56].

(3) Light wavelength and light intensity

The photochemical effect of light sources with different wavelength emitting ranges will have a profound effect on the photocatalytic reaction rate, depending on the types of photocatalysts. For $TiO_2$ photocatalysis, only UV irradiation can be used efficiently to decontamination due to the band gap energy [57]. Unfortunately, only 5% of the total irradiated natural sunlight has sufficient energy to cause effective photosensitization. Besides, energy loss due to light reflection, transmission and

12

energy loss as heating is inevitable during the photoprocess. This limitation largely invited more research on the application of $TiO_2$ to decontamination. Another factor limits photonic efficiency is the recombination between electron and hole. For these reasons, many approaches [58, 59] were applied to inhibit the recombination of electron and hole, and to enlarge the light wavelength of adsorption.

Photocatalytic reaction rate depends largely on the light absorption of the photocatalyst [35]. At low intensity, reactions involving electron-hole formation are predominant and electron-hole recombination is insignificant. At high intensity, the reaction rate was independent of light intensity, due to the recombination rate increase of electron-holes [60]. However, $TiO_2$ photocatalysis reaction rate is not highly dependent on light intensity, where a few photons of energy can sufficiently induce the surface reaction [57]. Theoretically, to achieve a high photocatalytic reaction rate, particularly in the complicated waste treatment, a relatively high light intensity is required to adequately provide each $TiO_2$ surface active sites. However, when light wavelength is larger than the absorption edge of approximately 387 nm, the surface reaction of $TiO_2$ particles without modifications is restricted.

## 1.5.4. Limitations and modifications for the application of $TiO_2$

$TiO_2$ heterogeneous photocatalysis has recently been the subject of numerous investigations as it is an attractive technique for the destruction of undesirable contaminants. For the waste activated sludge, however, there are mainly two problems

that are photocatalytic activity of $TiO_2$ and photocatalytic reactor. To improve the photocatalytic activity of $TiO_2$, modification of $TiO_2$ with noble metals, such as Pt and Ag [61], is widely used [62-64], owing to the several positive effects: (i) improvement of the electron-hole separation by trapping the electrons speeding up the formation of $O_2^{\bullet-}$, (ii) shift of light absorption into the visible-light range due to plasmon formation, (iii) modification of the surface adsorption properties of the photocatalysts and (iv) generation of hydroxyl radicals through the reaction with hydrogen peroxide produced by the noble metal deposits on photocatalyst [65].

To obtain efficient and appropriate photocatalytic reactor, catalyst-suspended photocatalytic reactor and catalyst-supported photocatalytic reactor were applied to degrade WAS, respectively. On the other hand, it is a tendency to use natural sunlight as the light source of $TiO_2$-based photocatalysis. Therefore, the light collector are researched widely [66, 67]. Compound parabolic collector (CPC) is deemed to be an efficient one with higher light reflection efficiency [68], but the structure of CPC is complicated which will increase the manufacturing cost. Thus, it is necessary to design a simple structure and high efficiency light collector.

1.5.5. Photocatalysis application in waste and wastewater treatment

Photocatalysis as an efficient wastewater treatment technology has been researched widely [39, 45]. During photocatalysis process, organic pollutants are photo-oxidized and heavy metal ions are photo-reduced. For a complete degradation of WAS,

however, some disadvantages are still remaining, such as catalyst separation from WAS for the catalyst-suspended photocatalysis, lower photocatalytic activity for catalyst-supported photocatalysis and requirement of special photocatalytic reactors.

## 1.6. Objectives and originality of this research

Anaerobic digestion is a very promising alternative treatment technology for waste activated sludge. When used in practice, however, its inefficiency and long retention time limits its application. This inefficiency is mostly contributed by excessive presence of refractory compounds which impede the anaerobic digestion in hydrolysis stage. The purpose of this study is to facilitate the hydrolysis of WAS by photocatalysis for anaerobic digestion of WAS and biogas production. The specific objectives are listed as follows:

(1) In order to realize the easy operation, economy and environmental protection, a catalyst-suspended photocatalytic reactor was developed to pretreat WAS before anaerobic digestion.

(2) To further improve the photocatalytic activity of the photocatalyst and decrease the cost of post-treatment, a catalyst-supported photocatalytic reactor with Ag-modified $TiO_2$ (AgX/$TiO_2$) as photocatalyst was developed.

(3) The performance of the catalyst-supported photocatalytic reactor in the degradation of WAS was to be investigated and the intermittent photocatalysis treatment was also to be examined in the anaerobic digestion process of WAS in a

photocatalytic anaerobic fermenter.

The originalities of this research are listed as follows.

(1) Photocatalysis was first applied for the pretreatment of WAS.

(2) Photocatalytic pretreatment was used to improve bio-hydrogen production from WAS.

(3) Intermittent photocatalysis treatment was used to solubilize WAS in the process of anaerobic digestion for improving biogas production.

## 1.7. Outline of the thesis

The outline of this research includes objective, methods, assessments and results, shown in Fig.1.4.
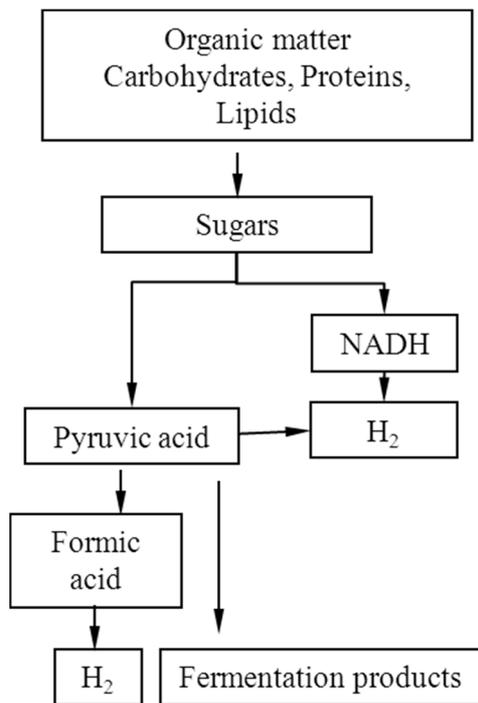
Fig. 1.1. Schematic representative pathways of fermentative hydrogen evolution from

waste activated sludge by anaerobic digestion [19]
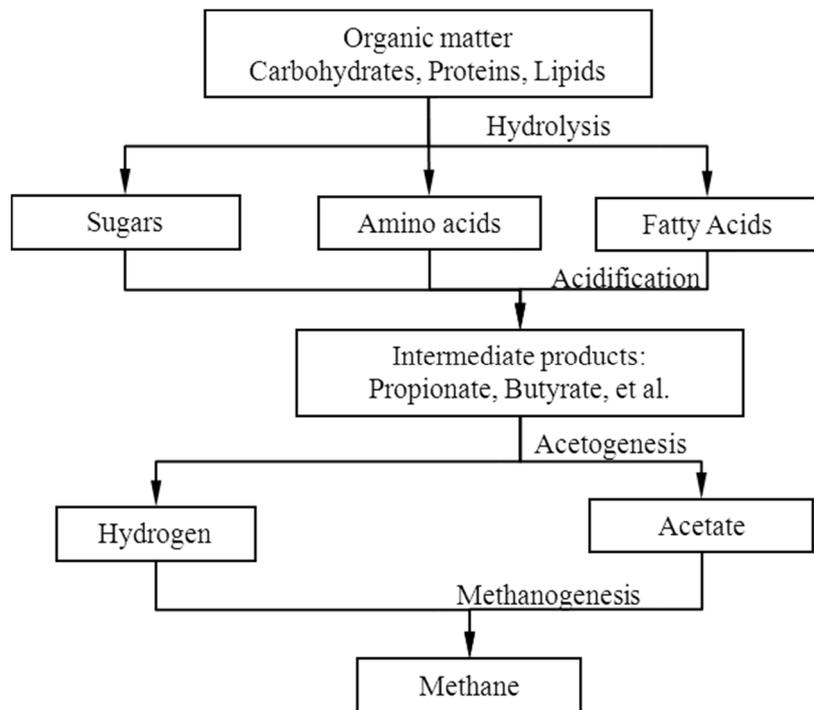
Fig. 1.2. Schematic representation of the decomposition of waste activated sludge by anaerobic digestion [20]
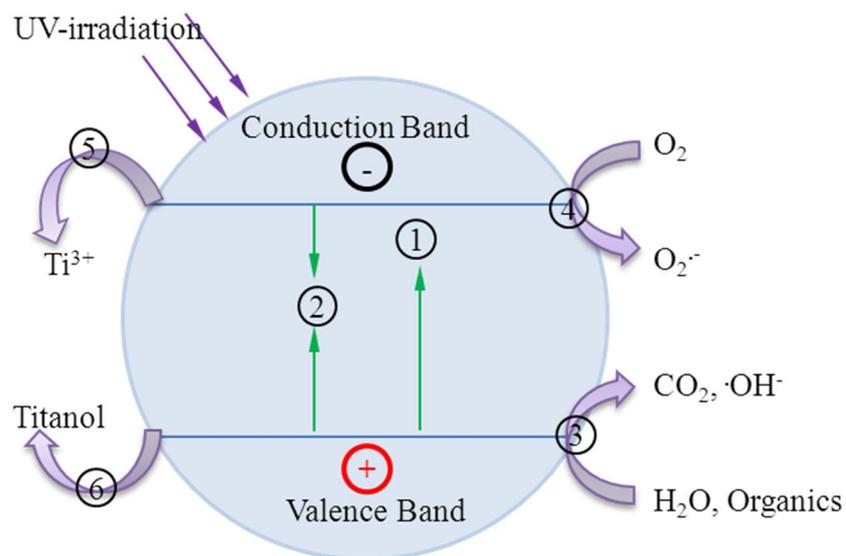
Fig.1.3. Schematic representation of the mechanism of $TiO_2$ photocatalysis and its main reactions [35, 69]. (① photogeneration of electron-hole pair, ② recombination, ③ oxidation of donor on the surface of $TiO_2$ particle, ④ reduction on the surface of $TiO_2$, ⑤ formation of $Ti^{3+}$, ⑥ formation of Titanol radicals )
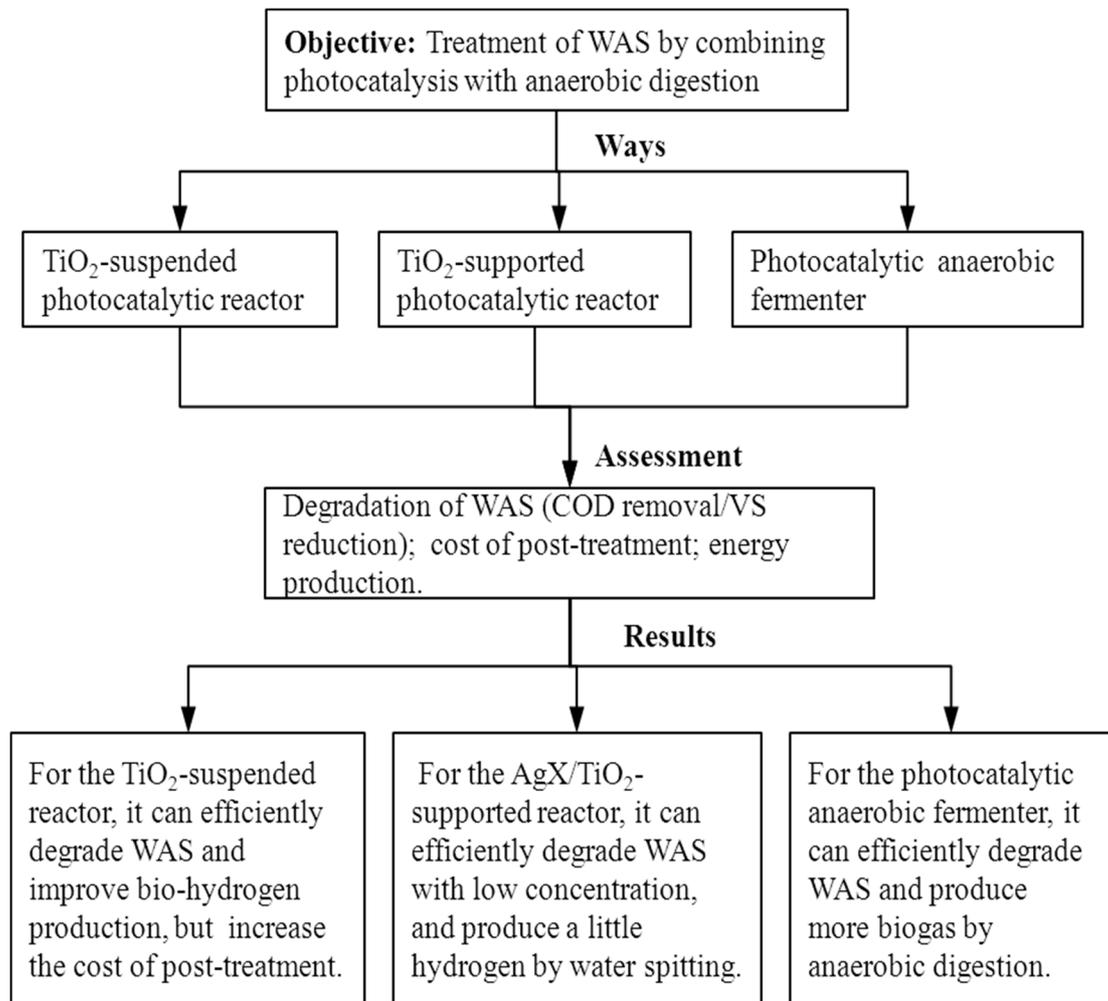
Fig.1.4. Outline of the thesis

# Chapter 2 Development of TiO$_2$-suspended photocatalytic reactor to pretreat WAS for improving bio-hydrogen production

## 2.1. Introduction

TiO$_2$-suspended photocatalytic reactor was widely used, due to its higher photocatalytic efficiency than TiO$_2$-supported photocatalytic reactor on the degradation of contaminants or waste [56, 70, 71]. However, very few photocatalytic reactors were developed to treat WAS and the photocatalytic pretreatment of WAS for hydrogen fermentation has not been studied as well. The objective of this study is to develop a novel photocatalytic reactor for the photocatalytic degradation of WAS. The parameters of the reactor and the operating conditions such as the shape of trough, circulating speed, TiO$_2$ dosage and initial concentration of WAS were optimized. Moreover, the experiment of hydrogen production using the photocatalysis pretreated WAS by anaerobic digestion was conducted.

## 2.2. Materials and methods

### 2.2.1. WAS, digested sludge and TiO$_2$

The WAS and digested sludge were collected from a sewage treatment plant in Ibaraki, Japan, and then kept at 4°C. For the adjustment of sloping trough circulating bed photocatalytic reactor (STCBPR), the raw WAS was diluted into different folds (0, 2.5, 5, 7.5, 10 and 15) using deionized water. For photocatalytic pretreatment and

21

anaerobic digestion experiments, the raw WAS was used directly without dilution. The characteristics of the WAS and digested sludge are listed in Table 2.1. As the data shown in Table 2.1, the ratio of volatile solids (VS) to total solids (TS) was very high, indicating that the main composition of sludge was organic matter. Meanwhile, the low ratio of soluble chemical oxygen demand (SCOD) to chemical oxygen demand (COD) demonstrates that most of COD was in the solid phase rather than the soluble phase. The catalyst used in this study was slurry of Degussa P-25 $TiO_2$ (Degussa AG, Germany), of which the physicochemical and optical properties and photocatalytic activity have been reported previously [72]. The zeolite used in this study was N.F.K. Natural Zeolite Powder NO.70 was from Gih Hwa Enterprise Co., Ltd, Japan.

2.2.2. Sloping trough circulating bed photocatalytic reactor

Considering the complicated composition and structure, the optical property (transmission, absorption and reflection of UV-light) and the photocatalytic requirements of WAS, STCBPR was developed. The schematic diagram of the experimental reactor is shown in Fig.2.1a. The reactor mainly consists of a rectangular plexiglass sloping flat with 10 troughs, a distributor with 10 holes drilled uniformly, a borosilicate glass cover, a 180 ml glass container, a magnetic stirrer (0-3000 r/min, PUREDU, CHINA), a UV-lamp and a peristaltic pump (0-1200 ml/min, GONGCHANG, CHINA). The flat is 18 cm in length, 12 cm in width and 0.6 cm in thickness. The effective illumination area of the flat was 150 $cm^2$. The 10 toughs were

fabricated uniformly on the flat at intervals of 1 cm. The length of the trough was 15 cm with 4 spherical bumps stuck at intervals of 3 cm. In order to obtain the optimal shape of through, three different shapes of the trough (rectangular, triangular and arc-shaped) were designed. The cross section of the trough is shown in Fig.2.1b. The spherical bump with rough surface was 3.5 mm in diameter. The spherical bump was made by mixing $TiO_2$ with the zeolite, kneading into sphere, then drying in oven (100 ℃, 3h), finally calcining (500 ℃, 2 h) in a muffle furnace (F-1404, Tokyo, Japan). The distributor was made of polymethyl methacrylate, and holes with diameter of 2.5 mm were drilled. The borosilicate glass cover could reduce the evaporation of the mixture and prevent the entry of impurities. The lamp was tubular UV-fluorescent lamp (Philips BM-15BLB) with an emission spectrum ranging from 320 to 410 nm and a peak of 370 nm. It was installed in parallel above the sloping flat to keep the light intensity uniform. The light intensity was detected by a portable photo-radiometer. The mixture of WAS and $TiO_2$ flowed continuously from the container to the sloping flat through a peristaltic pump. As control, an immersion-well photoreactor was used to pretreat WAS. The immersion-well photoreactor mainly consists of a container (180 ml) on a magnetic stirrer and a tubular UV-fluorescent lamp (Philips BM-15BLB). The pretreatment conditions were listed as follows: 1.5 mW/cm$^2$ of UV-light intensity, 1.5 g/l of $TiO_2$.

2.2.3. STCBPR adjustment and WAS photocatalytic pretreatment

STCBPR was adjusted to reach the optimum conditions for WAS degradation, and then used to pretreat WAS. Experiments of the STCBPR adjustment were carried out by varying four operating conditions (shape of the trough, circulating speed, $TiO_2$ dosage and dilution multiple of raw WAS). The STCBPR adjustment and WAS pretreatment experiments were conducted under to 1.5 mW/cm$^2$ of UV-light intensity. 150 ml of WAS and a certain amount of $TiO_2$ slurry was filled into the container, and the mixture (WAS and $TiO_2$) was stirred by a magnetic stirrer. Then, the peristaltic pump and UV lamp were turned on and the photocatalytic degradation experiments of WAS started. For the experiments of STCBPR adjustment and WAS pretreatment, the mixture was sampled every 2 h during 8 h treatment.

2.2.4. Bio-hydrogen production from photocatalysis pretreated WAS

Batch experiments for the bio-hydrogen production were carried out on three different kinds of WAS (photocatalysis pretreated WAS, UV-light pretreated WAS and raw WAS). Serum vials (total volume of 30 ml, SANSIN, JAPAN) were used as batch digesters. Each digester contained 22 ml of WAS and 5 ml of inoculum. Digested sludge was heated at 120 ℃ for 30 min to sterilize the hydrogen consuming bacteria and to enrich the hydrogen-producing bacteria [73], and then used as the inoculum for hydrogen fermentation. The initial pH of WAS and inoculum were adjusted to 5.7 using a diluted acid/alkali solution for hydrogen fermentation. All the digesters were

sealed with silica gel stoppers, and the nitrogen gas was purged to ensure an anaerobic condition. In addition, vials were wrapped by aluminum foil to avoid the substrate photolysis. The batch experiments were conducted at 37 ℃ for 4 days. All experiments were performed in triplicate with the average results being reported.

2.2.5. Analytical methods

Chemical oxygen demand (COD), soluble chemical oxygen demands (SCOD), total solid (TS), volatile solid (VS), and ammonia nitrogen ($NH_4^+$-N) concentrations were detected in accordance with the standard methods [74], and pH was determined by a SevenGo pro$^{TM}$ pH/Ion Meter (SG8, METTLER TOLEDO). For the fermentation experiment, the yield and content of the produced biogas were determined every 0.5 day during hydrogen fermentation process. The biogas was collected by two 10 ml plastic syringes, and the volume was read directly from the scale at the syringe. The gas composition was detected by a gas chromatography (GC-8A, SHIMAZU, Japan) equipped with a thermal conductivity detector (80 ℃) and a Porapak Q column (60 ℃), in which nitrogen was used as the carrier gas.

**2.3. Results and discussion**

2.3.1. Effect of trough shape on WAS degradation

The experiments were carried out by using STCBPR with three different shape trough (rectangular, triangular, and arc-shape) in order to attain the optimal one for the degradation of WAS. As shown in Fig.2.2a, the trough with arc-shape had a better

performance in the photocatalytic degradation of WAS than the other two with triangular or rectangular shapes. The removal rate of COD increased with time and the maximum removal rate of the three different reactors after 8 hours were 29.8%, 32.6% and 38.0%, respectively. The reduction rate of TS and VS are shown in Fig.2.2b. The reactor with arc-shape trough showed the highest removal of 37.0% (TS) and 40.0% (VS), followed by the rectangular one of 27.0% (TS) and 30.0% (VS), and the triangular one of 24.0% (TS) and 27.0% (VS). For the immersion-well photoreactor, TS and VS reductions and COD removal was only 5.2%, 7.3% and 6.6%, respectively.

When the mixture flowed in the rectangular trough at a certain circulating speed, it would flow along the walls of the rectangular trough, which reduced the light area of the mixture, resulting in the decrease of the photocatalytic efficiency. The triangular trough reactor increased the thickness of the mixture and decreased the surface area of the mixture on the sloping flat at the same circulation rate, which leaded to the reduction in light permeability and the decrease in illumination area, eventually reduced the photocatalytic efficiency. The arc-shape trough reactor had the advantages of uniform flow and larger illumination area, which was in favor of the photocatalytic degradation of the WAS. In addition, under the same circulation rate, the arc-shaped trough had a larger contact area with the mixture than the triangular and the rectangular ones. Moreover, the flow properties of WAS (as a non-Newtonian fluid), such as viscosity, plays a major role on oxygen transfer and mass transfer, which

consequently influences the hydrodynamic regime and the reactor performance [75, 76]. The shape of trough on the sloping flat would affect the motion of the mixture by changing the interaction force between the mixture and the trough. Therefore, the mixture flows in the trough, the value and direction of the interaction force change with different shapes, which directly leads to the change of mass transfer [77].

In addition, another advantage of the STCBPR is the design of spherical bumps in the trough. When the mixture flowed through the spherical bump in the arc-shape trough, a larger vortex was produced behind the spherical bump on account of different pressures between the front and behind part of the spherical bump. After comparison of the STCBPR with and without spherical bumps, the former showed higher efficiency for WAS degradation. The COD removal, TS and VS reduction rates increased by 5.9%, 4.0% and 6.0%, respectively (Fig. 2.2). The reason could be that the vortex further promoted the photocatalytic degradation of WAS by improving the mass transfer and the adsorption of oxygen. Hence, the following experiments adopted the arc-shape trough reactor with spherical bumps.

2.3.2. Effect of circulating speed on WAS degradation

For each circle, circulating speed influenced the photocatalysis time of WAS. Faster circulating speed shortened the photocatalysis time leading to the decrease of photocatalytic efficiency, while slower circulating speed extended photocatalysis time but increased operation cost instead. In addition, the mass transfer and fluid thickness

on the sloping flat changed as the circulating speed changes, which would influence the photocatalytic reaction. Therefore, it is necessary to investigate the circulating speed.

Experiments were carried out to test the effect of different circulating speeds (0, 175, 350, 525 and 700 ml/min), and the results are shown in Fig. 2.3. It can be seen that the COD concentration of the WAS decreased with time at any circulating speed. However, the removal rate of COD increased with circulating speed up to 350 ml/min. Further increase of circulating speed, i.e. > 350 ml/min, resulted in the decrease of removal rate of COD (Fig.2.3a). The TS and VS reduction (Fig.2.3b) had the same tendency with the COD removal rate. At the circulating speed of 350 ml/min, the highest TS and VS reduction and COD removal rate, TS and VS was 44.1%, 40.0% and 44.0%, respectively. The similar results of indole photocatalytic degradation in a circulating upflow reactor by UV/TiO$_2$ process were reported by Merabet et al. [78]. Ballari et al. [79] also reported that fast circulating speed improved the photocatalytic reaction by increasing mass transfer between WAS and TiO$_2$ catalyst and reducing the chances of agglomeration of catalyst particles. However, much faster circulating speed could reduce the illumination time, causing lower light energy to produce electron-hole pairs on the TiO$_2$ surface. In this study, the optimum circulating speed was determined to be 350 ml/min.

### 2.3.3. Effect of $TiO_2$ dosage on WAS degradation

As an important parameter, the catalyst dosage has been extensively studied on photocatalytic reaction [80]. In this study, the experiments of photocatalytic degradation of WAS were carried out under five different $TiO_2$ dosages (0 as control, 1, 2, 3 and 4 g/l). Fig.2.4a shows that along with the increase of $TiO_2$ dosage from 0 to 3 g/l, the photocatalytic degradation rate of WAS increased. However, the $TiO_2$ dosage of 4 g/l did not further enhance the removal rate. Jia et al. [56] reported a similar result about the degradation of landfill leachate by UV-$TiO_2$ photocatalysis. Compared with the $TiO_2$ dosage of 3 g/l, the COD degradation efficiency was 5.6 % lower at the $TiO_2$ dosage of 4 g/l (Fig. 2.4a). In addition, the removal efficiency of TS and VS was 7.3 % and 8.3 % lower, respectively (Fig. 2.4b). Therefore, the optimum $TiO_2$ dosage is 3 g/l in this study. At the optimum $TiO_2$ dosage, the maximum removal rates of COD, TS and VS were approximately 44%, 40% and 43%, respectively (Fig. 2.4b). The reason could be that $TiO_2$ was fully utilized when $TiO_2$ dosage was lower than 3 g/l, while not at higher dosage of 4 g/l. Moreover, redundant $TiO_2$ would decrease UV-light transmission and subsequently influence the photocatalytic degradation of WAS.

### 2.3.4. Effect of dilution multiple on WAS degradation

The dilution multiple of WAS would affect the concentration of the organic matter and the transmission of light into the mixture, so the optimal dilution multiple needs

to be determined. The experiments were carried out using the WAS in 0 as control, 2.5, 5, 7.5,10 and 15-fold dilution, and their effects on the degradation of WAS by STCBPR are shown in Fig.2.5. With the increase of dilution multiple, the rate of degradation increased. However, the absolute degradation decreased at high dilution multiple. According to the results and the operating cost, the optimum dilution multiple was in 7.5-fold dilution, and the removal rates of COD, TS and VS reached by 43.9%, 39.2% and 42.4% after 8 hours, respectively. Similarly, Tokumura et al. [81] reported that nearly 40% of mixed liquor suspended solids (MLSS) reduced after more than 24 h photo-Fenton treatment, and Yan et al. [82] reported that nearly 40% of MLSS reduced after 24 h heat-treatment as well. For comparison, the experiments of photocatalytic degradation of WAS using the immersion-well photoreactor were carried out. The results showed that WAS in 20-fold dilution could not be effectively degraded. Therefore, the STCBPR could overcome the negative effect of high concentration WAS, and the optimal dilution multiple is 7.5 for photocatalytic degradation of WAS.

2.3.5. Effect of photocatalysis on concentration of SCOD and $NH_4^+$-N

As shown in Table 2.2, the SCOD concentration of WAS increased as photocatalytic pretreatment time increased up to 6 hours. While the SCOD concentration decreased when the pretreatment time was beyond 6 hours. The highest SCOD concentration was 527.5 mg/L in 7.5-fold dilution. The reason could be as

follows: cellular and extracellular polymeric substances (EPS) in WAS were disintegrated, further the insoluble solid phase organics were converted into soluble organics [9, 83], and then partially degraded into $CO_2$ and $H_2O$. Other pretreatment methods, such as microwave, ultrasonic and thermal treatment, could also increase the SCOD concentration of WAS [84], but not effectively mineralize the organic matters in WAS [27, 85, 86]. Furthermore, microwave, ultrasonic and thermal treatment would consume more energy to dissolve the WAS. Thus comparably photocatalytic degradation of WAS was superior to other methods.

Compared to the initial concentration, $NH_4^+$-N concentration in WAS increased by 2.4 to 4.3 times under the designed dilution multiples. Little increase of ammonia from pretreated WAS by microwave was confirmed by Yu et al. [27]. The results demonstrated that the organics containing nitrogen, such as proteins and nucleic acid, were degraded by photocatalysis into small and soluble molecules. Feng et al. [87] also reported that the increase of $NH_4^+$-N concentration in WAS pretreated by ultrasonic was due to some organic nitrogen being released and subsequently hydrolyzed to ammonia. Therefore, the photocatalytic pretreatment could also improve the anaerobic digestibility of WAS on account of the increase of soluble carbon and nitrogen in the pretreatment process [24]. Based on the above results, the following experiments for hydrogen production were conducted via anaerobic digestion using photocatalysis pretreated WAS as substrate.

2.3.6. Effect of photocatalytic pretreatment on hydrogen production

In order to examine the effect of photocatalytic pretreatment time on the bio-hydrogen production, the hydrogen fermentation experiments were conducted using the pretreated WAS. The photocatalytic pretreatment time was 0 h, 2 h, 4 h, 6 h, 8 h respectively under the condition of 3 g/l of $TiO_2$, 350 ml/min of circulating speed, 1.5 mW/cm$^2$ of UV-light and arc-shaped trough with spherical bumps. The experimental results showed that the maximum hydrogen production from pretreated WAS was in the range of 31.6 to 53.2 ml-$H_2$/l-sludge at the photocatalytic pretreatment time of 2 to 8 h (Fig.2.6a), while the maximum hydrogen production from raw WAS was only 3.1 ml-$H_2$/l-sludge. In addition, the hydrogen production firstly increased with the pretreatment progressing, but it began to decrease when the pretreatment time was longer than 6 h. The reason could be that longer pretreatment time caused superfluous degradation of soluble organics by photocatalysis [88]. Consequentially, the decrease of soluble organics resulted in the reduction of hydrogen production. The optimal photocatalytic pretreatment time was 6 h.

Fig.2.6b and Fig.2.6c showed the cumulative hydrogen production and the hydrogen concentration from the three different kinds of WAS: photocatalytic pretreatment WAS, UV-light pretreatment WAS and raw WAS (control). The cumulative hydrogen production of the three samples increased with time, and the highest hydrogen production was obtained on the second day. The WAS treated by photocatalysis achieved the highest cumulative hydrogen production (53.2

ml-$H_2$/l-sludge) and the highest concentration of hydrogen (70.6%). The cumulative hydrogen production from photocatalysis pretreated WAS was 3.6 times higher than that of UV-light pretreated WAS, and 17 times higher than that of raw WAS. In addition, the maximum hydrogen concentration from photocatalysis pretreated WAS was 1.94 times higher than that of UV-light pretreated WAS, and 22.6 times higher than that of raw WAS. These results indicated that photocatalysis pretreatment could enhance bio-hydrogen production from WAS via anaerobic digestion, while UV-light irradiation pretreatment showed little improvement. The other pretreatment methods (such as heating and microwave) could also improve solubilization of organic material, but they had different effect on hydrogen production by anaerobic digestion, using the pretreated WAS as substrate. Microwave and heating could efficiently enhance hydrogen production but consumed large amounts of energy. Moreover, Carrère et al. [29] reported that heating pretreatment increased final effluent color and ammonia inhibition. Guo et al. [89] reported that microwave could extract toxic matters such as heavy metal ions. These toxic matters would restrain the hydrogen production bacteria to some extent. Thus, the photocatalytic pretreatment technology could serve as a more attractive pretreatment way for the degradation of refractory organics and then increased bio-hydrogen production. Another bio-hydrogen production experiment was carried out by using the WAS as substrate pretreated in an immersion-well photoreactor for 6h. The cumulative hydrogen production was 23.2 ml-$H_2$/l-sludge with hydrogen concentration of 38.6%. The cumulative hydrogen

production and the hydrogen concentration were lower than from the WAS pretreated by STCBPR, which was 53.2 ml-$H_2$/l-sludge and 70.6%, respectively. Therefore, the STCBPR could be a better reactor to solubilize the organic matters in WAS, and eventually improve the bio-hydrogen production.

## 2.4. Conclusions

It is confirmed that the STCBPR is effective in degrading WAS. Moreover, it is easy to be operated and maintained. As a result, nearly 45% of COD and 47% of VS reduction were obtained in 7.5-fold dilution after reaction for 8 h. In addition, photocatalytic pretreatment could increase the SCOD and $NH_4^+$-N concentrations of the WAS. Moreover, photocatalysis pretreated WAS as substrate produced the maximum hydrogen via anaerobic digestion, followed by UV irradiation pretreated WAS. Therefore, the STCBPR could be a better reactor for WAS pretreatment when taking bio-hydrogen production into consideration.

Table 2.1. Compositions of waste activated sludge (WAS) and digested sludge (DS)

| Parameters | WAS | DS |
|---|---|---|
| Chemical oxygen demand (COD, mg/l) | 16249 | 14360 |
| Soluble chemical oxygen demand (SCOD, mg/l) | 1752 | 500 |
| SCOD/COD (%) | 10.8 | 3.5 |
| Total solids (TS, mg/l) | 7483 | 8630 |
| Volatile solids (VS, mg/l) | 5606 | 5130 |
| VS/TS (%) | 74.8 | 59.4 |
| Ammonia nitrogen ($NH_4^+$-N, mg/l) | 132.6 | 280 |
| pH | 6.83 | 7.2 |

Table 2.2. SCOD and $NH_4^+$-N concentrations of waste activated sludge with different dilution multiple after photocatalytic pretreatment process (unit: mg/l)

| Photocatalytic pretreatment time (h) | SCOD | | | $NH_4^+$-N | | |
|---|---|---|---|---|---|---|
| | 5-fold dilution | 7.5-fold dilution | 10-fold dilution | 5-fold dilution | 7.5-fold dilution | 10-fold dilution |
| 0 | 312 | 210.2 | 159.1 | 23.5 | 16.7 | 8.9 |
| 2 | 348.8 | 308.9 | 259.2 | 28.6 | 18.9 | 13.1 |
| 4 | 469.2 | 485.6 | 308.8 | 40.8 | 28.3 | 25.4 |
| 6 | 502.6 | 527.5 | 402.6 | 50.9 | 55.1 | 34.7 |
| 8 | 452.1 | 421.9 | 279.2 | 56.2 | 60.3 | 38.6 |
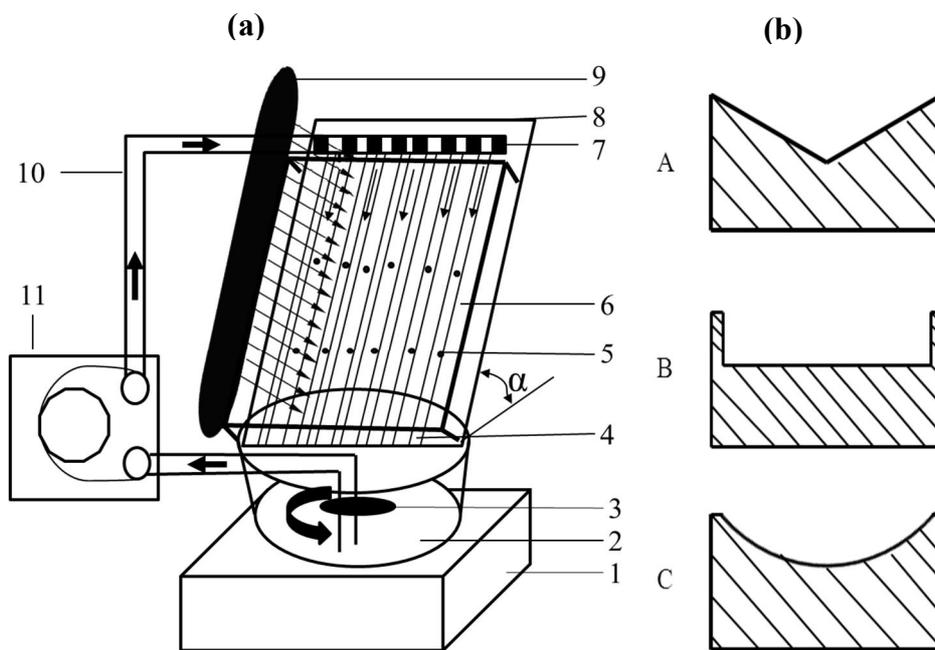
Fig.2.1. Schematic of sloping trough circulating bed photocatalytic reactor (a) and the schematic of trough shape (b). (1 Magnetic stirrer; 2 Container; 3 Rotor; 4 Trough; 5 Spherical bump; 6 Glass cover; 7 Distributor; 8 Sloping flat; 9 UV-lamp; 10 Fluid flow pipe; 11 Peristaltic pump. A Triangular shape; B Rectangular shape; C Arc-shape)
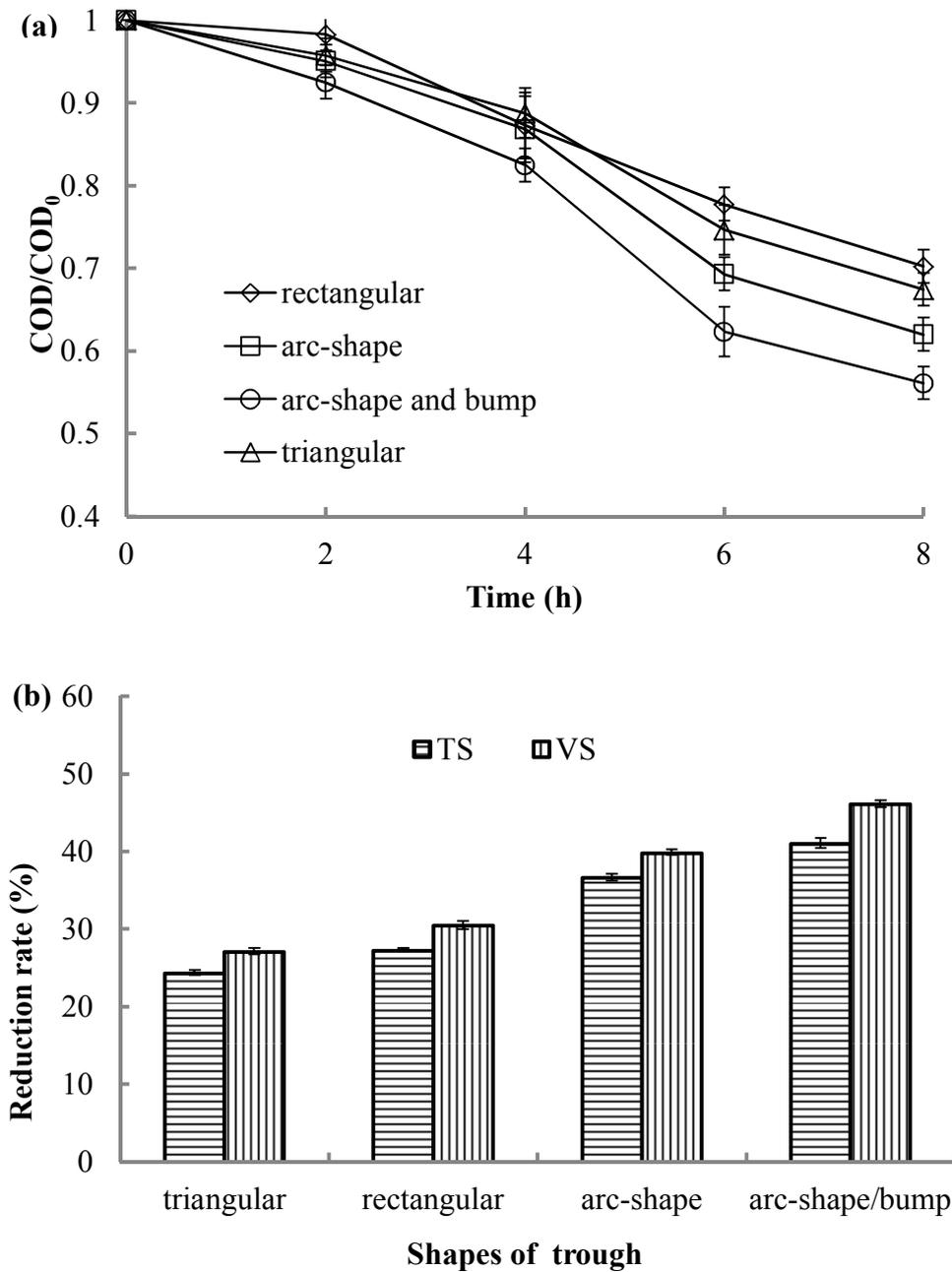
Fig.2.2. Effect of trough shapes on COD removal (a) and TS/VS (b) reduction during photocatalytic degradation of WAS. (TiO$_2$ dosage = 3 g/l, Circulating speed = 350 ml/min, UV-light intensity =1.5 mW/cm$^2$, Dilution multiple = 7.5-fold, Reaction time = 8 h)
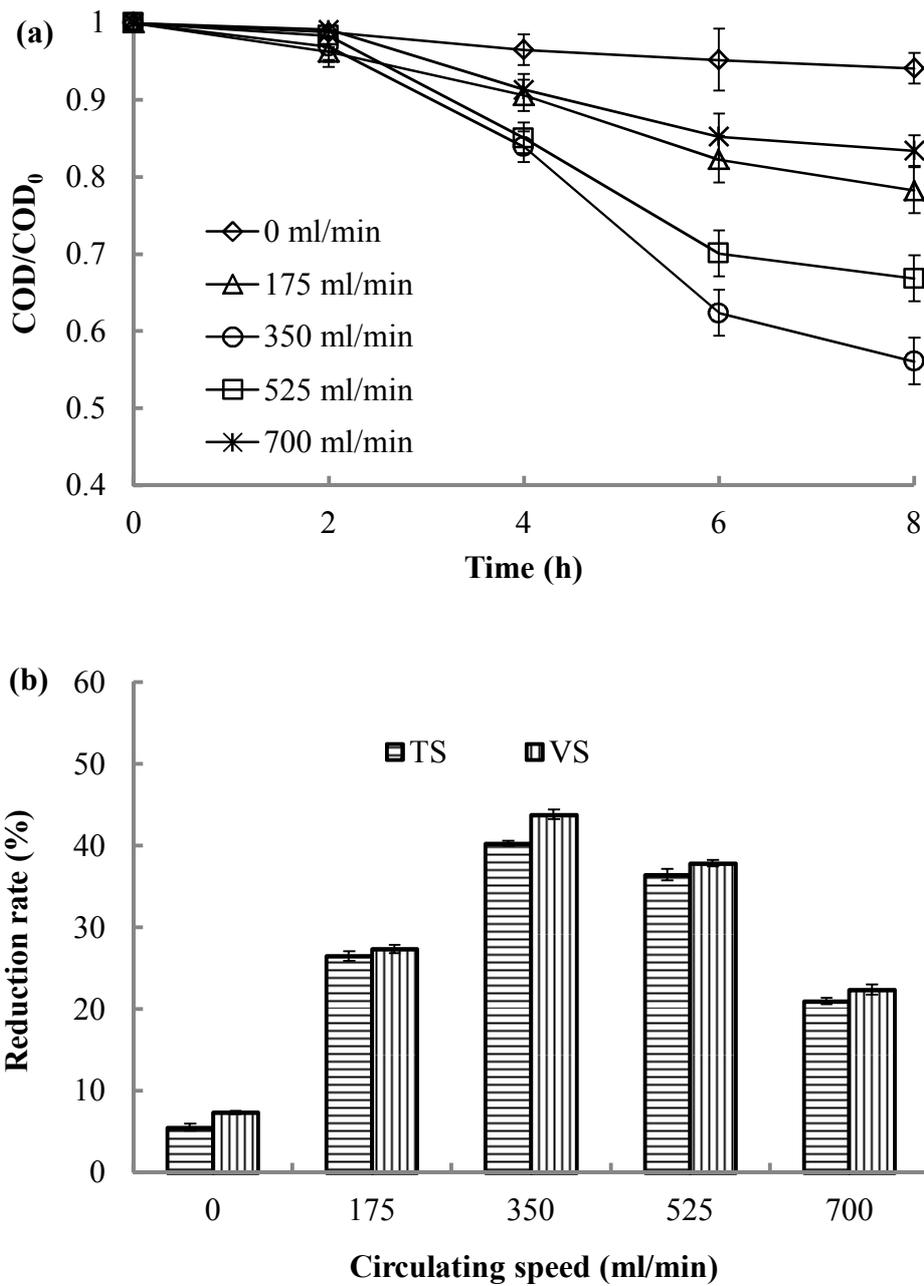
Fig.2.3. Effect of circulating speeds on COD removal (a) and TS/VS reduction (b) during photocatalytic degradation of WAS. (TiO$_2$ dosage = 3 g/l, UV-light intensity = 1.5 mW/cm$^2$, Dilution multiple = 7.5-fold, Reaction time = 8 h)
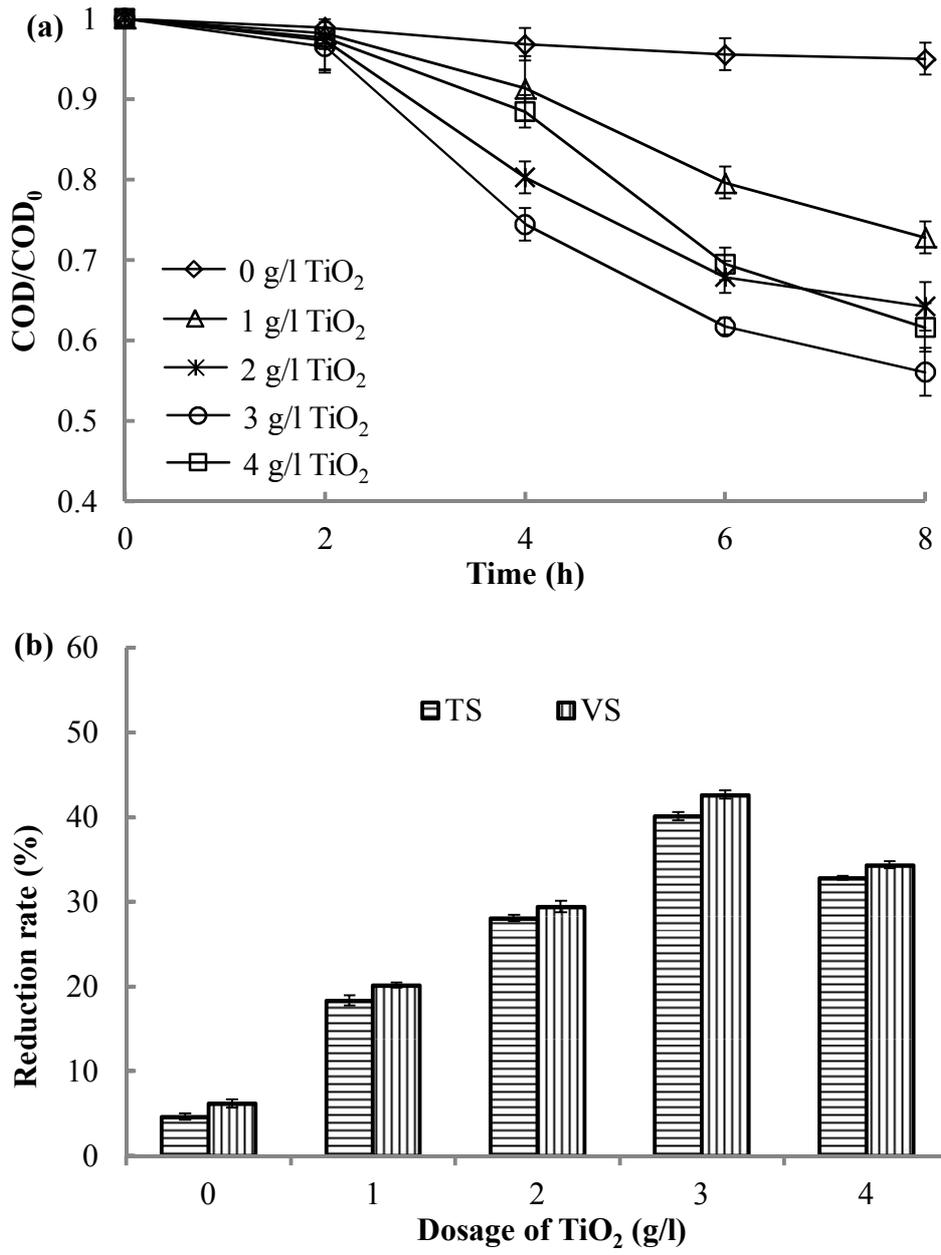
Fig.2.4. Effect of TiO$_2$ dosage on COD removal (a) and TS/VS (b) reduction during

photocatalytic degradation of WAS. (Circulating speed = 350 ml/min, UV-light

intensity = 1.5 mW/cm$^2$, Dilution multiple = 7.5-fold, Reaction time = 8 h)
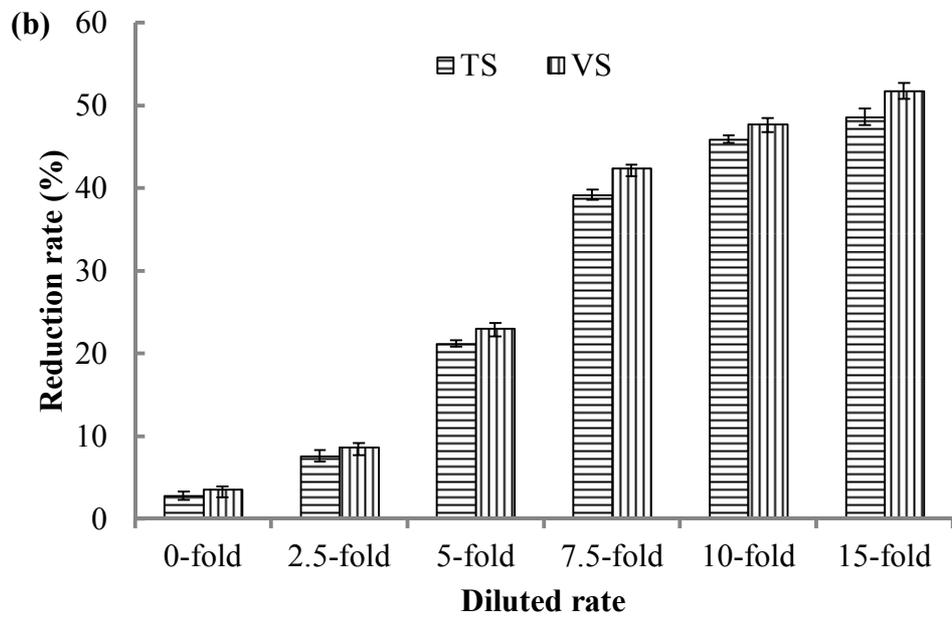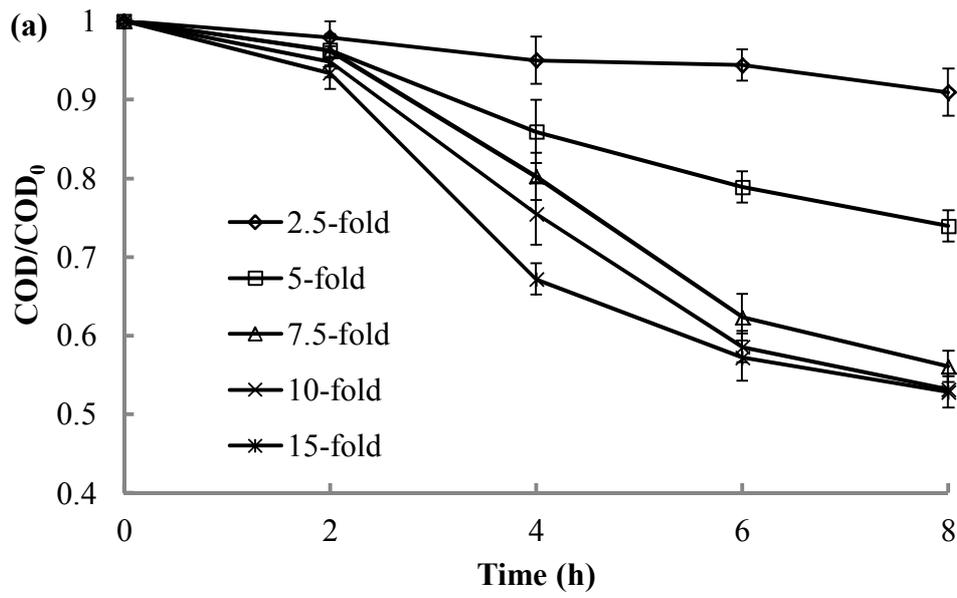
Fig.2.5. Effect of dilution multiple on COD removal (a) and TS/VS reduction (b) during photocatalytic degradation of WAS. (Circulating speed = 350 ml/min, $TiO_2$ dosage = 3g/l, UV-light intensity = 1.5 mW/$cm^2$, Reaction time = 8 h)
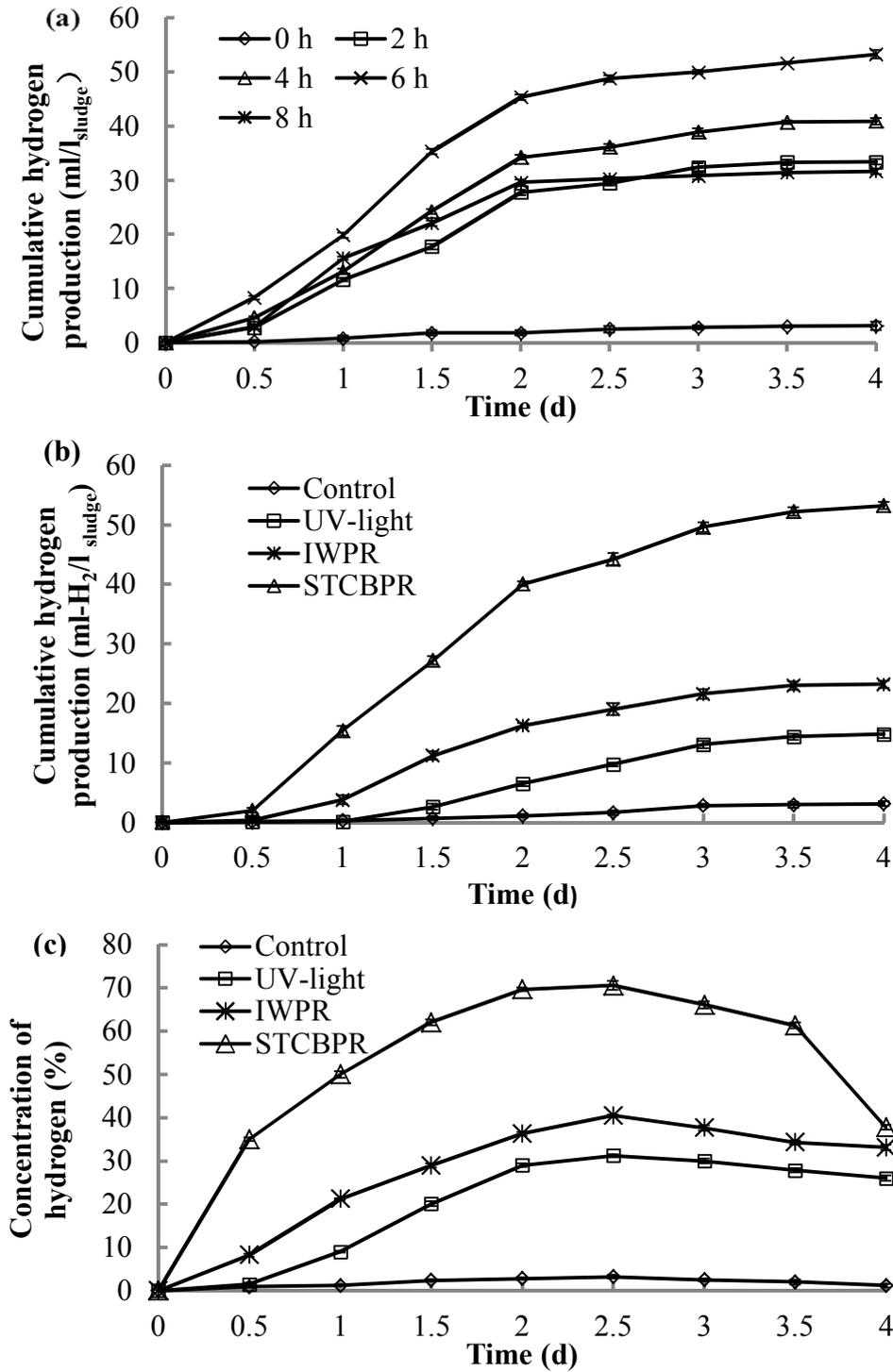
Fig.2.6. Effect of different photocatalytic time on hydrogen production (a), Cumulative hydrogen production of three different WAS (b), and Hydrogen concentration of three different WAS (c).

42

# Chapter 3 Development of TiO$_2$-supported photocatalytic reactor for WAS degradation and hydrogen production

## 3.1. Introduction

From the results of Chapter 2, it is clear that catalyst-suspended type reactor could improve the hydrogen production from pretreated WAS, but it enlarged the volume of WAS, and increased the cost of photocatalyst separation from WAS. Therefore, catalyst-supported reactor was focused in this chapter to overcome the shortages. On the other hand, to enhance the biodegradability of WAS by catalyst-supported reactor, the photocatalytic activity of the catalyst need to be improved. Therefore, photocatalyst with high activity and catalyst-supported reactor need to be developed to fulfill this research gap.

The objective of this chapter is first to synthesize the photocatalyst of Ag-Ag$_2$O-AgCl/TiO$_2$ (AgX/TiO$_2$), then to develop a new solar fluidized tubular photoreactor (SFTPR) with transparent AgX/TiO$_2$ film to treat WAS for 72 hours. The feasibility of photocatalysis and performance of the new photocatalytic reactor on the photocatalytic degradation of WAS and hydrogen production were also discussed. Moreover, this research is also committed to providing a useful reference for the practical application of photocatalysis on the WAS degradation and the design of photocatalytic reactor.

**3.2. Materials and methods**

3.2.1. Photocatalytic reactor

The schematic diagram of the SFTPR is shown in Fig.3.1a. The reactor mainly consisted of a bracket, a collector (L×W = 15 cm×20 cm), 10 glass tubes (L×D = 18 cm×1 cm), a peristaltic pump (0-1200 ml/min, GONGCHANG, CHINA), a container (750 ml), a magnetic stirrer (0-1200 r/min, PUREDU, CHINA), and pipes. The illuminated volume of the glass tubes was about 250 ml. The 10 glass tubes, joined with plastic tubes, were coated with $AgX/TiO_2$ film on the inner walls. The $AgX/TiO_2$ film coated on glass tubes had high photo-permeability efficiency. The reactor was sealed for collecting the hydrogen. The light collector, made of aluminum foil shown in Figs.3.1b and 3.1c, consisted of 10 modules, and each module composed of a slope reflecting surface and a level reflecting surface. When sunlight irradiated on the slope reflecting surfaces, the light was reflected into the tubes by the slope reflecting surface. The transmitted ray would also be reflected into the tubes by the level reflecting surface as the sunlight was transmitted to the tubes.

3.2.2. Preparation of $AgX/TiO_2$ film coated on the glass tubes

(1) Preparation of the glass tubes before coating on the glass tubes

The cleanliness of tubes directly affects the adhesive strength and uniformity on the inner wall of the tubes: the higher cleanliness, the stronger adhesive strength and

higher uniformity. In this study, the tubes were firstly washed by neutral detergent and ethanol (Wako, 99.5%) for 3 times, and then immersed in sulfuric acid (Wako, 98%) for 12 h. After that the tubes were flushed off using deionized water and dried at 100 ℃ in an oven for later use.

(2) Preparation of $TiO_2$ film on the glass tubes

The cleaned tubes were placed vertically, and then the slurry of $TiO_2$ was spread on the inner wall using a high-velocity stream (600ml/min/cm$^2$) which could make the film enough uniform and thin. This process could ensure the tubes to bear stress evenly during calcination process then obtain a high quality $TiO_2$ film. After about 1 h, the supernumerary $TiO_2$ slurry flowed down along the inner wall with only a piece of thin film of $TiO_2$ kept to the inner wall of the glass tube. When the $TiO_2$ film became dried, the tubes were put into oven (100 ℃) to dry further for 2 hours. Finally, after being calcined at 400 ℃ for 2 h in a muffle, the coated tubes were cooled naturally to room temperature. These tubes were labeled as $TiO_2$ film-coated tubes.

(3) Preparation of $AgX/TiO_2$ on the glass tubes

The photocatalyst were prepared using the modified impregnation-precipitation-photoreduction method [65]. Firstly, washed the $TiO_2$ film-coated tubes with deionized water to wipe off the supernumerary $TiO_2$ powder then immersed them into HCl solution (0.025, 0.05, 0.1 or 0.2 mol/l) for 30 min. After that, these tubes were dried in oven (60 ℃) for 1 h then cooled at room temperature. Secondly, the tubes were immersed into 0.025, 0.05, 0.1 or 0.2 mol/l $AgNO_3$ solutions for 10 min. Then,

these tubes were dried in oven (60 ℃) for 1 h and cooled at room temperature. Thirdly, the glass tubes were calcined at 400 ℃ for 2 h to obtain the AgX/TiO$_2$ film. Finally, the glass tubes were irradiated with an ultraviolet lamp (Philips BM-15BLB) for 1 h to reduce partial Ag$^+$ ions in the form of AgCl particles to Ag$^0$ species by photochemical decomposition of AgCl.

### 3.2.3. WAS degradation and simultaneous hydrogen production

WAS used in this study was collected from a sewage treatment plant in Ibaraki, Japan, and then kept at 4 °C. The initial characteristics of WAS were as follows (g/l except pH): pH 6.7, total solid (TS) 4.0, volatile suspended solid (VSS) 3.2, chemical oxygen demand (COD) 8.7, respectively. The TiO$_2$ used in this study was a TiO$_2$ slurry (STS-21, Ishihara Sangyo Kaisha, LTD. Japan) with characteristics as pH 8.3, absorbance of 0.43, viscosity of 42.2 mP•s and particle size of 20 nm given by the manufacturer. The experiment was carried out on a roof in Tsukuba, Ibaraki, Japan (latitude 36° 6' N, longitude 140° 6' E) in September 2012. The Mean visible/UV (290–390 nm) light intensity was measured with a portable UV light meter (Custom UV340, TAIWAN of CHINA) shown in Fig.3.2.

The WAS was designed to flow directly from one tube to another connected in series and finally to the container, and then returned to the tubes by the peristaltic pump (100 ml/min). The container was continuously stirred (300 r/min) by a magnetic stirrer to achieve a homogeneous suspension. Samples and hydrogen production were

collected once per 6 hours (9 a.m. and 3 p.m.) during the 72 h treatment. Blank assay without catalyst and only $TiO_2$ film catalyst were also carried out in parallel.

## 3.2.4. Characterization of photocatalyst

X-ray powder diffraction (XRD, Bruker D5005 diffractometer, Cu Kα radiation, scan range 2θ between 10 and 90°, 40 kV, 30mA) was used to identify the crystalline phases present, and also used to estimate the relative change of sample crystallinity and the average crystallite size of $Ag^0$, $Ag_2O$ and AgCl nanoparticles. Field emission scanning electron microscopy (FE-SEM, Hitachi S-4700 FE-SEM, secondary electron imaging mode, accelerating voltage 2 kV, beam current 10 μA, working distance 3mm) was used to observe the morphology of $TiO_2$ film and $Ag^0$, $Ag_2O$ and AgCl nanoparticles deposited on $TiO_2$ film surface.

## 3.2.5. Analytical methods

Chemical oxygen demand (COD), volatile solids (VS) and total solids (TS) concentrations were detected in accordance with the standard methods [74], and pH was determined by a pH Meter (SG8, METTLER TOLEDO). The yield and content of the produced gas were determined every day during photocatalytic degradation process. The volume of gas was checked by the syringe. The gas composition was detected by a gas chromatography (GC-8A, SHIMAZU, JAPAN) equipped with a thermal conductivity detector (80 ℃) and a Porapak Q column (60 ℃), in which

nitrogen was used as the carrier gas.

## 3.3. Results and discussion

3.3.1. Photocatalyst characterization

Figure 3.3a showed the XRD patterns of pure $TiO_2$ (1) and $AgX/TiO_2$ (2) samples. The XRD patterns indicated that anatase was the only crystalline phase of $TiO_2$ in the pure $TiO_2$ sample. The presence of Ag diffraction lines were clearly detected at approximately 22.74° and 85.57°(2θ) for the $AgX/TiO_2$ sample, including AgCl (chlorargyrite) at approximately 27.66°, 46.119° and 76.58° (2θ) and $Ag_2O$ at approximately 32.118° and 57.34° (2θ) (peaks marked by arrowhead in Fig.3.3a), respectively.

SEM images of pure $TiO_2$ and $AgX/TiO_2$ samples are shown in Figs.3.3b and 3.3c. Figure 3.3b showed that the pure $TiO_2$ displayed a high degree of size and shape heterogeneity, with spherical particles ranging from 25 nm to as large as 40 nm in accordance with the results of Pulido Melián et al. [90]. Figure 3.3c indicated that the deposition of AgX had no effect on the surface structure and shape of $TiO_2$. The distribution of AgX on the surface of $TiO_2$ was not uniform. The $AgX/TiO_2$ was observed as aggregates on the surface of $TiO_2$ with different size and irregular shape.

3.3.2. Effect of $AgNO_3$ concentration on the activity of $AgX/TiO_2$

Different concentrations of $AgNO_3$ (0, 0.025, 0.05, 0.1 or 0.2 mol/l) were tested for

Ag doping on $TiO_2$ to obtain its optimum concentration. The concentrations of HCl used were the same as the $AgNO_3$ solution in the experiment, and methyl orange (MO, 25 mg/l) was used as the target organics. The results (Fig.3.4a) showed that MO degradation rate increased from 30.6% to 99.5% with $AgNO_3$ concentration increased from 0 to 0.1mol/l, and this increase trend stopped when further increased the $AgNO_3$ concentration to 0.2mol/l, about 90.5% of MO removal at this concentration. Therefore, the optimal concentration was about 0.1mol/l in this study, and almost 100% MO was degraded, higher than the result (about 91%) obtained by Wang et al. [91]. This observation was probably brought about by low silver loadings on $TiO_2$ surface (Fig.3.3c), which is advantageous for the enhancement of the electron-hole separation and surface electron excitation by plasmon resonances. According to van Grieken et al. [92] excessive surface coverage by the silver deposits could reduce the access of radiation to the $TiO_2$ surface and block the $TiO_2$ active sites as well.

3.3.3. Improvement of light collector on the activity of $AgX/TiO_2$

The comparative tests were performed between the new photocatalytic reactor with and without light collector under the same operation conditions (solar radiation and flow velocity). Figure 3.4b shows the MO degradation difference when $AgX/TiO_2$ (0.1 mol/l $AgNO_3$) was used as catalyst. Almost 100% degradation of MO could be achieved after 2 h photocatalytic treatment by the reactor with collector, while only 92.5% for the reactor without collector. This improvement was mainly attributed to

49

the increase of accumulated light energy per unit volume as compared to the system without light collector. The amount of accumulated light energy was proportional to the reflection efficiency of the slope reflecting surfaces. When sunlight irradiated on the slope reflecting surfaces, the light would be reflected into the tubes. Based on the design parameters (data not shown), about 90% of the glass tube surface could be irradiated (Fig.3.1c), and the light intensity could increase by about 26% after reflection when compared to the same reactor without collector. The improvement brought about by light collector was not high, about 7.5% in MO degradation rate. However, the newly-developed reactor was still promising due to its effectiveness in solar energy collection. In addition, it was simple, easy-maintained, low-cost and ease of processing. Therefore, it was used in the following experiments.

3.3.4. Effect of AgX/TiO$_2$ on WAS degradation of and hydrogen production

(1) Effect of AgX/TiO$_2$ on the photocatalytic degradation of WAS

Figure 3.5a shows the degradation of WAS in the photocatalytic reactor with pure TiO$_2$ and AgX/TiO$_2$ as catalyst, respectively. The degradation of WAS by AgX/TiO$_2$ photocatalysis was much higher than by TiO$_2$ photocatalysis, which were 69.1% and 45.3% for COD removal in 72 h, respectively. The degradation rate (absolute COD removal per hour, in mg/l/h) of WAS was about 73.5 mg/l/h and 54 mg/l/h at the first 24 h, then gradually increased to 87.7 mg/l/h and 64.7 mg/l/h at the 72$^{th}$ h. Both supernatants of WAS faded and became clear with their color changed from

black-grey to earth-yellow after $AgX/TiO_2$ and $TiO_2$ photocatalysis degradation for 18 h and 30 h, respectively. The color fading of WAS could increase light permeability and then enhanced the photocatalysis efficiency for WAS degradation.

(2) Effect of $AgX/TiO_2$ on the photocatalytic hydrogen production

Figure 3.5b shows the hydrogen production from WAS by pure $TiO_2$ and $AgX/TiO_2$, respectively. It should be noted that no hydrogen were detected during the 72 h photolysis process of WAS without catalyst. About 7866.7 μmol-$H_2$/L-sludge was obtained after $AgX/TiO_2$ photocatalysis of WAS for 72 h, in contrast to 1863.1 μmol-$H_2$/L-sludge production from $TiO_2$ photocatalysis of WAS. The significant increase of hydrogen yield was attributed not only to the AgX loading on $TiO_2$ enhancing electrons-holes separation but also to the improved thermo-dynamical possibility for hydrogen production by photocatalytic water splitting [93]. Specifically, the Fermi level of $TiO_2$ is higher than that of Ag. When Ag is deposited on the surface of $TiO_2$, electrons can be transferred from $TiO_2$ to Ag then reach the same Femi level, leading to the formation of Schottky barrier. The Schottky barrier can trap electrons efficiently, resulting in the separation of electrons-holes, thus enhance the photocatalytic activity. Thermodynamically, the formation of $AgX/TiO_2$ could improve water splitting to produce hydrogen and oxygen, which is attributable to the much lower conduction band potential of $AgX/TiO_2$ than the hydrogen electrode potential, and also to the higher valence band potential of $AgX/TiO_2$ than the oxygen electrode potential. In addition, little change was found for the hydrogen production

51

rate during the whole photocatalytic degradation of WAS, about 127.7 and 25.8 $\mu$mol-$H_2$/L-sludge/h in average for AgX/$TiO_2$ and $TiO_2$ photocatalysis, respectively. The result also implied that hydrogen could come from water splitting by photocatalysis on the inner wall of the glass tubes.

3.3.5. Comparison with other pretreatment methods

Several other sludge treatment technologies have been compared with respect to WAS degradation, volume reduce, odor and color removal, energy consumption, operation and environmental protection. The advantages and disadvantages of these treatments are listed in Table 3.1. Thermal treatment [29, 31, 94], microwave [95] and ultrasonic [24] could act as a new technology to treat WAS, but their high energy consumption is the biggest obstacle. Anaerobic digestion technology [17, 94] is an economic and sustainable way to treat WAS but needs long retention time, while aerobic digestion could efficiently degrade WAS within a relatively short retention time with relatively high energy consumption. Photocatalytic technology [72, 88, 96, 97] may overcome the above-mentioned disadvantages and simultaneously remove odor, color and heavy metal ions, and produce hydrogen by photocatalytic water splitting. This study presents a new photocatalysis reactor with AgX/$TiO_2$ film coated, and the preliminary results obtained indicate that the reactor has potential for WAS treatment and simultaneous $H_2$ production in the near future.

## 3.4. Conclusions

The photocatalyst of AgX/TiO$_2$ film was synthesized successfully, and its photocatalytic activity was significantly improved due to silver and silver compound (Ag$_2$O-AgCl) doping on TiO$_2$. The light collector was also simple and effective on enhancing the photocatalytic activity of the photocatalyst. For the treatment of WAS, 69.1% of COD removal and 7866.7 µmol-H$_2$/L-sludge were achieved in SFTPR with AgX/TiO$_2$ as photocatalyst in 72 h, which was 50% and 350% higher than in SFTPR with TiO$_2$ as photocatalyst.

Table 3.1. Comparison of photocatalytic technology with other commonly applied sludge treatment methods.

| Treatment method | Experimental conditions | Advantages | Disadvantages | References |
|---|---|---|---|---|
| Heating | 121 - 180 ℃, 20-60min，600-2500kPa | Improve the solids hydrolysis rate, reduce sludge volume, increase $H_2$ yield. | Increase final effluent color and ammonia inhibition, high energy consumption. | [29, 89, 98] |
| Acid | Adjust the solution to pH=2, then to pH=7 | Low-cost, easy to operate, high metal-binding capacities. | Low selectivity, produce inhibitors, time consuming. | [9, 99] |
| Alkaline | 8 g NaOH/100 g TS-sludge, 20min-60min | Low-cost, easy to operate, high metal-binding capacities, increase hydrogen yield. | Low selectivity, produce waste products, higher concentration inhibition. | [28, 29] |
| Microwave | 560 w × 2 min; 850W × 3min | Significantly reduce sludge volume and processing time, no chemical addition, no harmful by-products, increase hydrogen yield. | Destruct microorganisms non-selectively, higher energy consumption, extract heavy metal ions from sludge. | [89, 95] |
| Ultrasonic | 2 w/ml × 5 min; 5000 kJ/kg TSS×5 min | Effectively improve organics solubilization, less retention time, reduce sludge volume, less harmful by-products. | Fail to reduce VS, frequently replace the ultrasound probes, extract heavy metal ions, reduce hydrogen yield | [89, 100] |
| Enzyme | 0.6% (w/w, enzyme/TS-sludge), 40-50 ℃, 4 h | Easy to control, no harmful by-products; enhance solid reduction, increase hydrogen yield. | Limitation of accessible surface area and enzyme adsorption. | [32, 101] |
| Photocatalysis | 20W lamp, $TiO_2$ of 20 mg/l, and 96 h | Remove efficiently heavy metals and organic pollutant, low energy consumption, environmental-friendly. | Time consuming, low efficiency of supported photocatalyst. | [96, 102] |
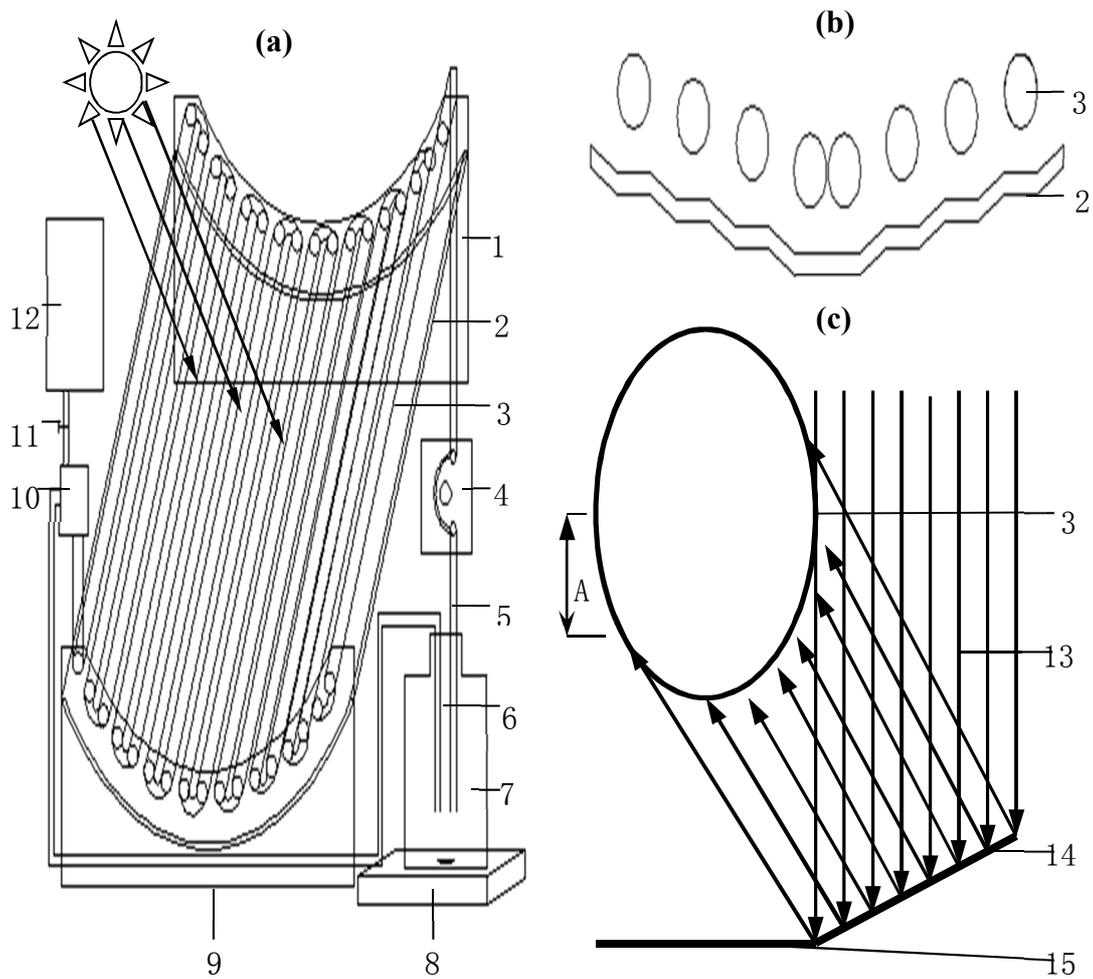
Fig.3.1. Schematic of solar fluidized tubular photocatalytic reactor (SFTPR) (a), cross-sectional view of the light collector (b), partial enlarged detail of light collector and glass tube (c). (1 Upper bracket, 2 Light collector, 3 Glass tube, 4 Peristaltic pump, 5 Outlet, 6 Inlet, 7 Container, 8 Magnetic stirrer, 9 Lower bracket, 10 Buffer unit, 11 Switch, 12 Hydrogen collecting bag, 13 Sunlight, 14 Slop reflecting surface, 15 Level reflecting surface)
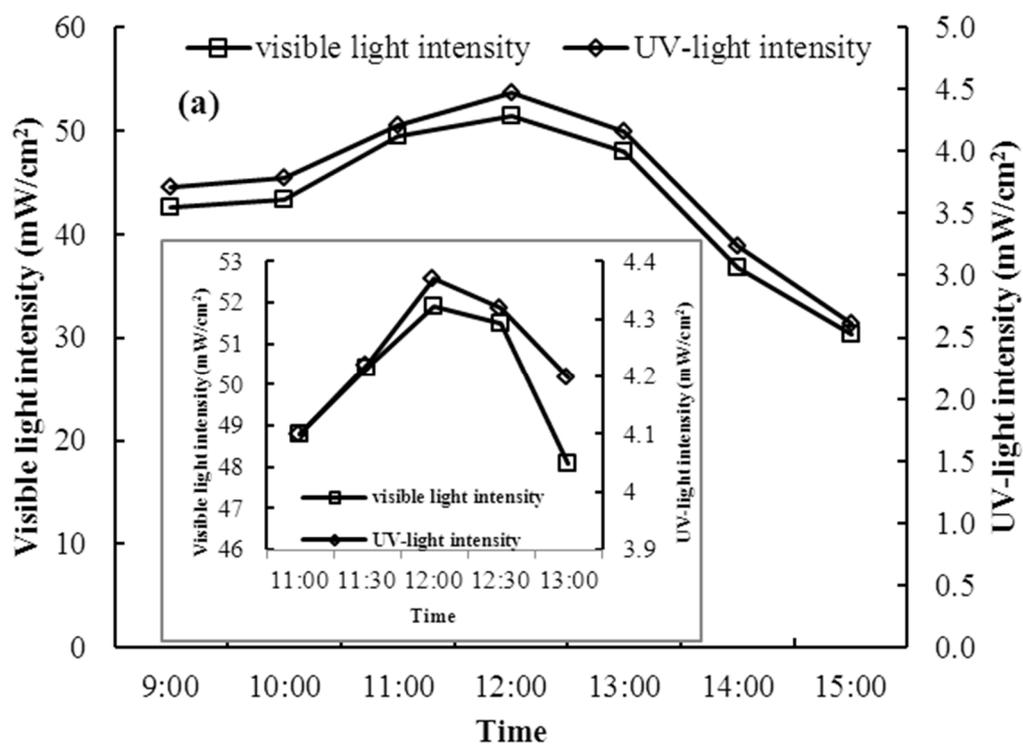
Fig.3.2. Mean visible/UV light intensity used for WAS degradation and hydrogen production (a), the visible/UV light intensity used in the experiments for methyl orange degradation (b).
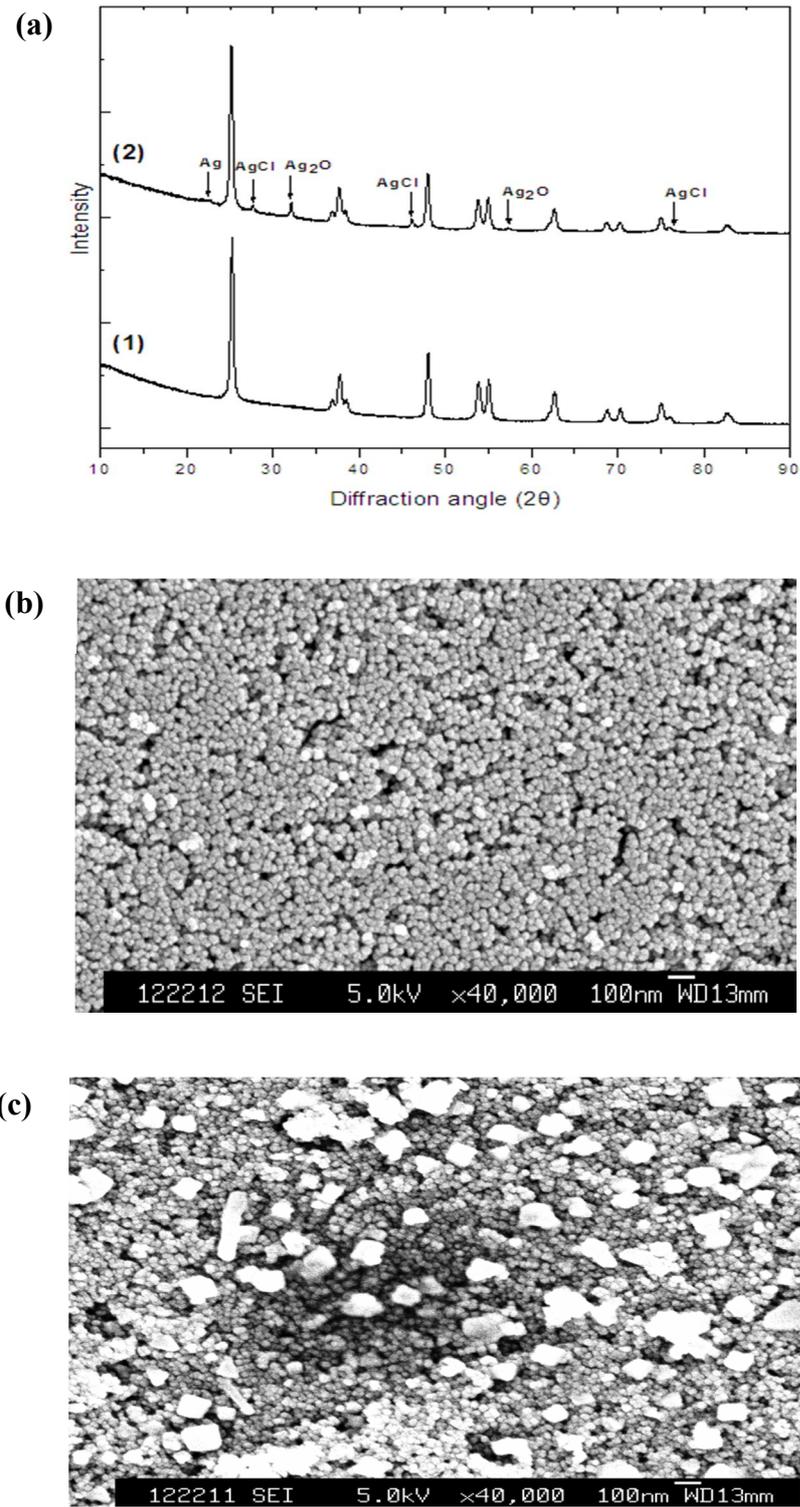
Fig.3.3. XRD patterns of pure $TiO_2$ (1) and $AgX/TiO_2$ (2) samples (a), SEM images of

pure $TiO_2$ (b) and $AgX/TiO_2$ samples (c).
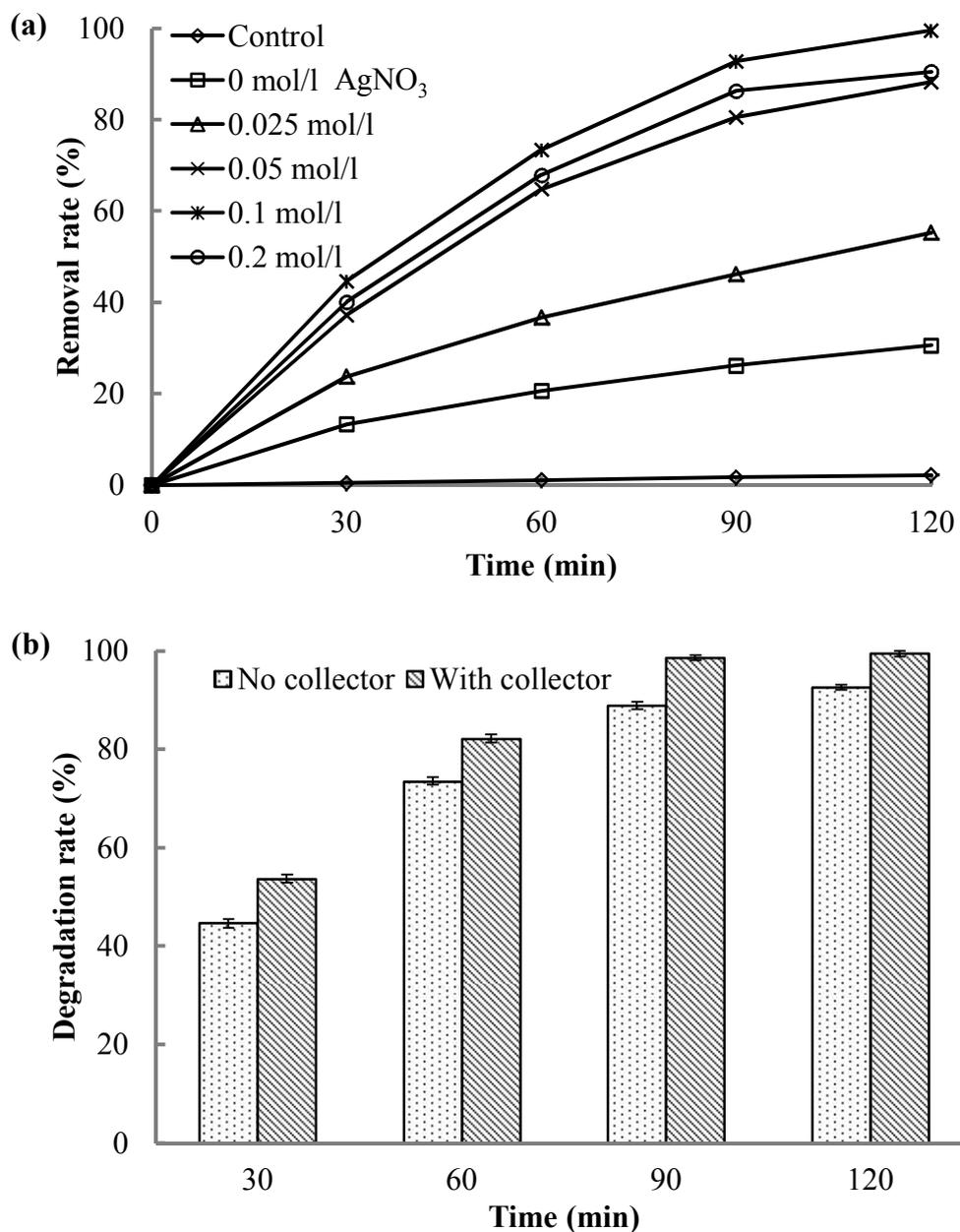
Fig.3.4. Effect of AgNO$_3$ concentration on the photocatalytic activity of AgX/TiO$_2$ for

methyl orange (MO) degradation (a), effect of collector on the photocatalytic activity

of AgX/TiO$_2$ for the degradation of MO (b). Control refers to the condition that is no

catalyst only light irradiation.

58
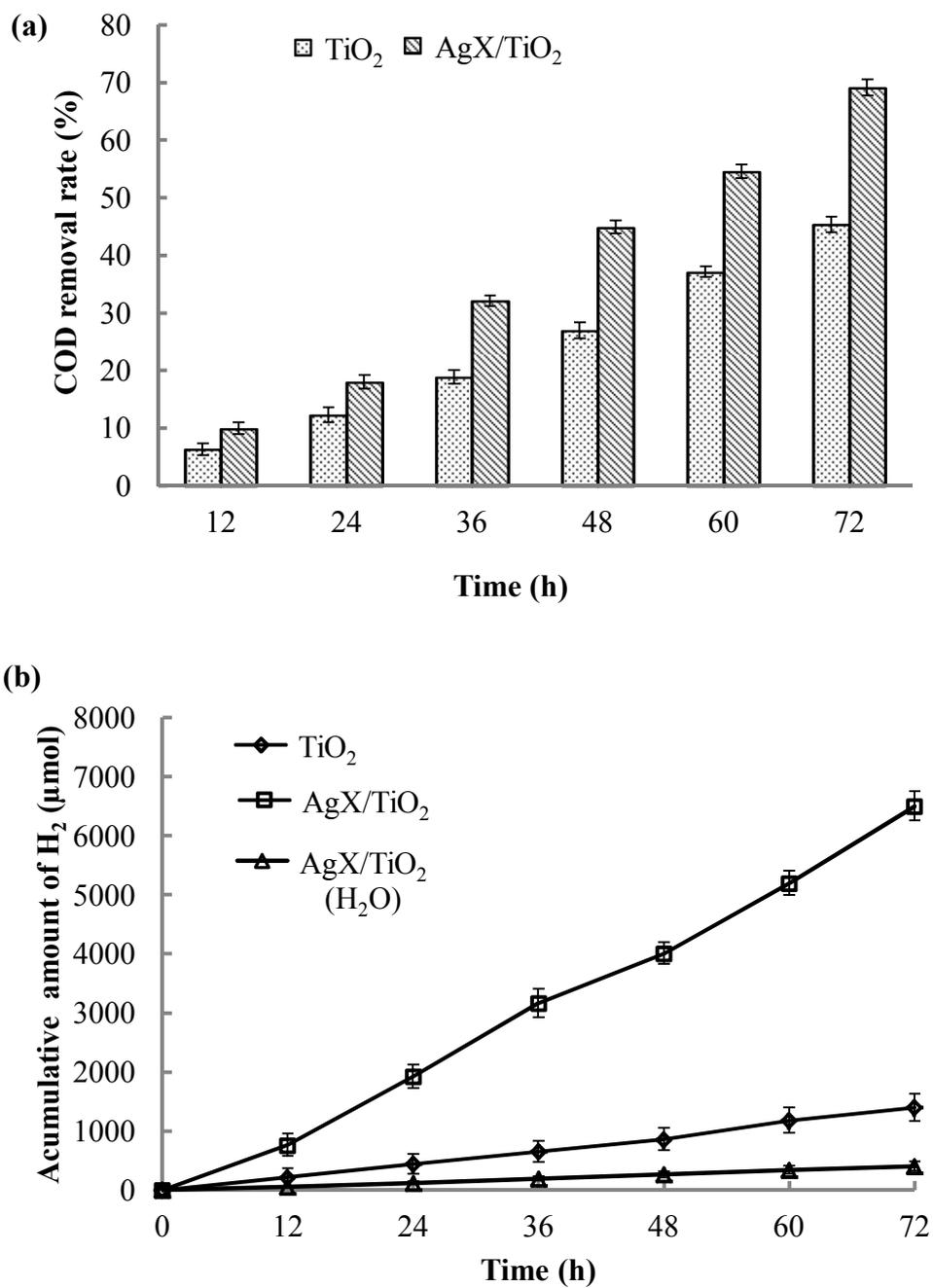
Fig.3.5. Degradation of WAS by $TiO_2$ photocatalysis and $AgX/TiO_2$ photocatalysis, respectively (a), hydrogen production from WAS by $TiO_2$ photocatalysis and $AgX/TiO_2$ photocatalysis, respectively (b).

# Chapter 4 Development of photocatalytic anaerobic fermenter for WAS degradation and simultaneous biogas production

## 4.1. Introduction

On the base of the previous study (Chapter 3), $TiO_2$-based photocatalysis could degrade WAS efficiently while with a little hydrogen production. However, there are several points needed to reconsider: (i) the solar photocatalytic reactor occupies large land area, (ii) long retention time is still needed for photocatalytic degradation, and (iii) the treated WAS contains many organics which can be further used as a source of energy, such as biogas. Therefore, in this chapter, the combination of photocatalysis and anaerobic digestion was studied for the treatment of WAS.

The objective of this chapter is to intermittently pretreat WAS by $TiO_2$ photocatalysis and produce methane from the WAS via anaerobic digestion simultaneously in a photocatalytic anaerobic fermenter. As we know, $TiO_2$ photocatalysis is no-selective, i.e. it solubilizes the WAS while influences the activities of microorganisms in WAS. Therefore, in order to decrease its negative effect, some tests were carried out in the photocatalytic anaerobic fermenter to obtain the optimal photocatalysis time. First, for obtaining the optimal photocatalytic condition, a preliminary experiment was carried out to check the changes of SCOD and adenosine triphosphate (ATP) concentration of WAS after photocatalytic

60

pretreatment for various intervals in the photocatalytic anaerobic fermenter. Then, methane production from WAS in the photocatalytic anaerobic fermenter was conducted under the optimal conditions. Finally, the mechanisms for the enhancement of methane production from photocatalytic anaerobic fermenter were investigated from the aspect of organic compounds conversion in the WAS.

## 4.2. Materials and methods

4.2.1. WAS, digested sludge and photocatalyst

The WAS and digested sludge (DS) were collected from a sewage treatment plant in Shimodate, Ibaraki, Japan, then kept at 4°C. The characteristics of the WAS are shown in Table 4.1. The high VS/TS ratio indicates that the main components of sludge are organic substances. The low ratio of soluble chemical oxygen demand (SCOD)/chemical oxygen demand (COD) demonstrates that most COD was insoluble and entrapped in the solid phase. For the methane anaerobic digestion experiment, the digested sludge was used as seeding sludge (15%), and its' compositions are shown in Table 4.1, too. Before used as seed inoculums, the digested sludge was cultivated in a water bath at 35 ℃ for 20 days to be acclimated to the mesophilic anaerobic digestion used in this study. The $TiO_2$ used in this study was the $TiO_2$ (STS-21, Ishihara Sangyo Kaisha, LTD. Japan). The characteristics were as follows: pH 8.3, Absorbance 0.43, Viscosity 42.2 mP•s, Particle size 20 nm.

61

### 4.2.2. Photocatalytic reactor

The schematic diagram of the experimental reactor is shown in Fig.4.1. The volume of the reactor was 1.2 L, with a biogas gathering port and an extract port, a magnetic stirrer (0-1200 r/min, PUREDU, CHINA). It mainly consisted of photocatalytic unit and methane production unit. For the photocatalytic unit, it consisted of a UV-lamp (15W, Philips) and a cylindrical glass cover (12 cm in length, 6 cm in diameter) coated with diaphanous $Ag/TiO_2$ film on the external wall. For the methane production unit, a cylindrical dummy plate (18 cm in length, 8 cm in diameter) with many holes (1 cm indiameter) installed between the cylindrical glass cover and the wall of reactor. The holes could offer sufficient mass transfer. The cylindrical dummy plate was sticked with aluminum foil on the inside wall. The aluminum foil was used to shade the UV-light.

### 4.2.3. Preliminary experiments

1.2 L WAS was pretreated in the photocatalytic anaerobic fermenter for 10 h, under the conditions of temperature of 35 ℃, UV-light intensity of 0.7 $mW/cm^2$ and constant stirring by a magnetic stirrer (PUREDU, CHINA). Samples were taken out at 2, 4, 6, 8 and 10 h to analyze the changes of SCOD and adenosine triphosphate (ATP) in WAS, and then to obtain the effect of photocatalysis on SCOD and negative effect on microorganisms. With the results, an optimal photocatalytic time was obtained for the following experiments.

### 4.2.4. Batch anaerobic digestion for methane production

The experiment of methane production from WAS was conducted in the photocatalytic fermentation reactor with the optimal photocatalysis time. The control experiment was performed using the same reactor under the same conditions, but without photocatalytic treatment. The initial pH of substrate was adjusted to 7.0 with sodium hydroxide (NaOH). After injecting nitrogen to create anaerobic condition, the reactors were put into a temperature-controlled water-bath (35 ℃) for 35 days. The biogas production was measured per day by plunger displacement method. The fermentation medium was sampled at the initial and end of methane fermentation process for the measurement of pH, TS, VS, COD and SCOD.

### 4.2.5. Analytical methods

COD, SCOD, TS, VS were detected in accordance with standard methods [74], and pH was determined by a digital pH meter (Metter-Toledo Group). ATP value was detected using a BacTiter-Glo™ Microbial Cell Viability Assay (Promega, USA).The biogas was collected using three 50 ml plastic syringes, and the volume was read directly by the scale on the syringe. The biogas compositions (hydrogen, methane and carbon dioxide) were determined by gas chromatography (GC-8A, SHIMAZU, JAPAN) equipped with a thermal conductivity detector (80 ℃) and a Porapak Q column (60 ℃), in which nitrogen was used as the carrier gas.

## 4.3. Results and discussion

4.3.1. Effect of photocatalysis on the SCOD and ATP of WAS

WAS pretreatment can be evaluated by the changes of SCOD concentrations to observe the effectiveness of pretreatment methods. On the other hand, methanogens can only consume directly soluble organics to produce methane. SCOD concentration as an indicator reflects the content of soluble organics in WAS. Therefore, in this part of the study, SCOD concentrations were analyzed and compared with those of untreated control sludge samples. Figure 4.2 shows the changes of SCOD concentration in WAS during photocatalytic process for 10 h. The SCOD concentration increased from 1087.2 mg/l to 1451.6 mg/l with photocatalytic time increase from 0 h to 8 h, while decreased to 1372.8 mg/l after pretreatment for 10 h. This result could be attributed to that photocatalysis could solubilize the solid organics into soluble organics and simultaneously degrade the soluble organics into carbon dioxide and water [103, 104]. Therefore, the optimal photocatalytic time was 8 h in this study with respect to SCOD changes.

On the other hand, ATP, as an indicator of metabolically active cells and an index of microbial density [105], was tested per 2 h during the photocatalysis process for 10 h. The changes of ATP concentration in WAS is shown in Fig.4.3. The ATP concentration increased from 1.44 to 1.57 µg/mg-VSS after photocatalysis for 2 h, and then decreased to 1.53 µg/mg-VSS at 4 h and 1.38 µg/mg-VSS at 6 h. The result

indicates that transitory photocatalysis did not reduce but slightly increase the ATP concentration, while long period of photocatalysis had negative effect on microorganisms and even inactivated them due to photocatalytic oxidation. Having a similar mechanism of inactivation, low dose ozone treatment could increase ATP concentration but high dose ozone treatment decrease ATP concentration [106]. Considering the changes of SCOD and ATP in WAS during photocatalytic process, the optimal photocatalytic time was set at 4 h in this study.

4.3.2. Improvement of intermittent photocatalysis on $CH_4$ production

To investigate the actual photocatalytic improvement on methane production from WAS, anaerobic digestion experiments were carried out using WAS as substrate in the photocatalytic anaerobic fermenter and the control fermenter (without photocatalysis). The yields and contents of methane are shown in Figs.4.4a and 4.4b, respectively. The accumulative $CH_4$ production was 1266.7 ml-$CH_4$/L-sludge and 923.2 ml-$CH_4$/L-sludge in the photocatalytic anaerobic fermenter and the control fermenter, respectively. It could be seen that the start-up period was shortened (about 3 days) in the photocatalytic anaerobic fermenter. After the start-up period, biogas production increased gradually to a daily maximum of 105 ml/l on day 10, and the corresponding methane content increased from 18% to 71%. Thereafter, biogas production gradually decreased until day 21 then slightly increased, and finally decreased, but the methane content remained stable at about 70% until day 28. However, the start-up period was 7

days in control, and the maximum daily biomass yield was 84.2 ml-$CH_4$/L-sludge on day 19. In addition, little hydrogen production was detected during the whole anaerobic process in photocatalytic anaerobic fermenter, and only occurred in the first 3 days in the control fermenter (data not shown). It was confirmed that little hydrogen was produced during the initial hydrogen fermentation stage in the two fermenters. On the other hand, continuous hydrogen production in photocatalytic anaerobic fermenter was obtained by photocatalytic water splitting [107]. It can be concluded the photocatalytic anaerobic fermenter exhibited better performance than the control fermenter in terms of shortened start-up period and higher biogas yield.

### 4.3.3. Improvement of intermittent photocatalysis on WAS degradation

The degradation of WAS was expressed by COD removal. Fig.4.5 shows the initial and final COD values in the two fermenters. About 60.5% of COD removal from 12.7 g/l to 5.0 g/l was obtained in the photocatalytic anaerobic fermenter, while only 43.5% of COD removal from 12.7 g/l to 7.2 g/l in the control fermenter. The removal rate of COD increased gradually, with the highest removal rate of 563 mg COD/l/day and 445.4 mg COD/l/day from day 15 to day 20, after that decreased to 47.4 mg COD/l/day and 55 mg COD/l/day from day 20 to day 25 in the photocatalytic anaerobic fermenter and the control fermenter, respectively. The result obtained here on COD removal indicated that the sludge quantity was reduced significantly after anaerobic digestion in both reactors. Moreover, more removal in the photocatalytic

66

anaerobic fermenter was obtained than in the control fermenter, implying that intermittent photocatalytic pretreatment enhanced the degradation of WAS via anaerobic digestion.

## 4.4. Conclusions

It is confirmed that photocatalytic anaerobic fermenter was effective in degrading WAS. Moreover, it was easy to be operated and maintained. As a result, 60.5% of COD removal and 1266.7 ml-CH$_4$/L-sludge were obtained during anaerobic digestion and intermittent photocatalytic treatment. While only 43.5% of COD removal and 932.2 ml ml-CH$_4$/L-sludge were obtained in the control fermenter. Therefore, it is confirmed that intermittent photocatalytic treatment could enhance the WAS degradation and methane production in the anaerobic digestion process of WAS. Moreover, the photocatalytic anaerobic fermenter could be a better reactor for WAS degradation and methane production and provides a useful reference for the practical application of photocatalysis in WAS treatment.

Table 4.1. Characteristics of waste activated sludge (WAS) and digested sludge (DS)

| Items | WAS | DS |
|---|---|---|
| Chemical oxygen demand (COD, mg/l) | 12753 | 14080 |
| Soluble chemical oxygen demand (SCOD, mg/l) | 1027 | 530 |
| Total solids (TS, mg/l) | 6903 | 8845 |
| Volatile solids (VS, mg/l) | 5686 | 5196 |
| Volatile suspended solids (VSS, mg/l) | 4640 | 4036 |
| pH | 6.80 | 7.23 |
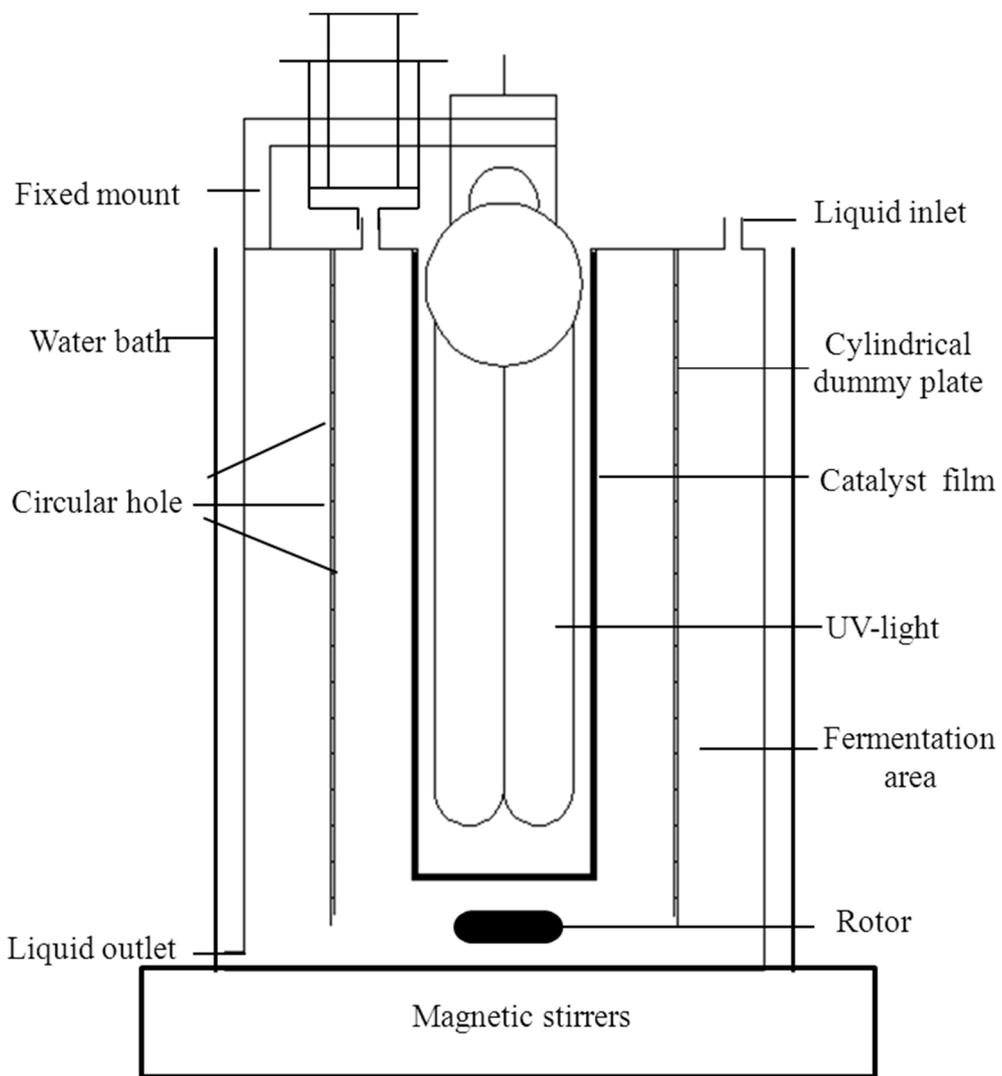
Fig.4.1. Schematic of the photocatalytic-anaerobic digestion reactor
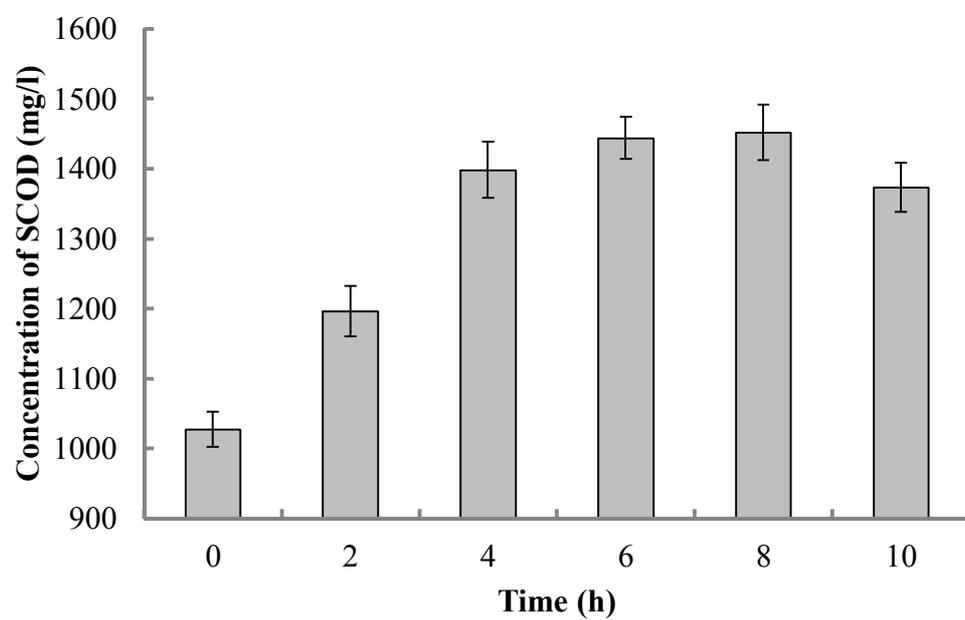
Fig.4.2. Changes of SCOD during photocatalytic degradation of WAS
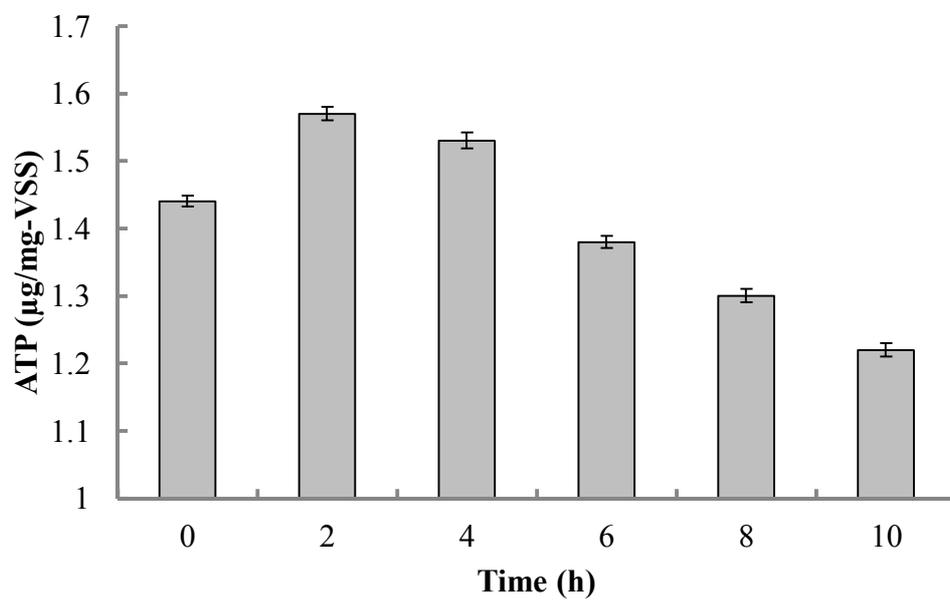
Fig.4.3. Changes of ATP during photocatalytic degradation of WAS
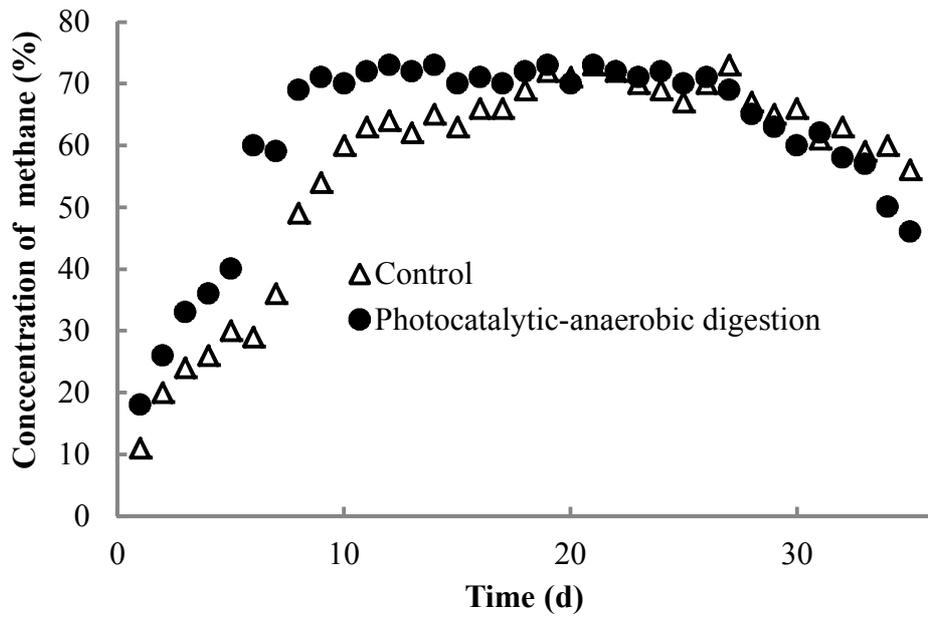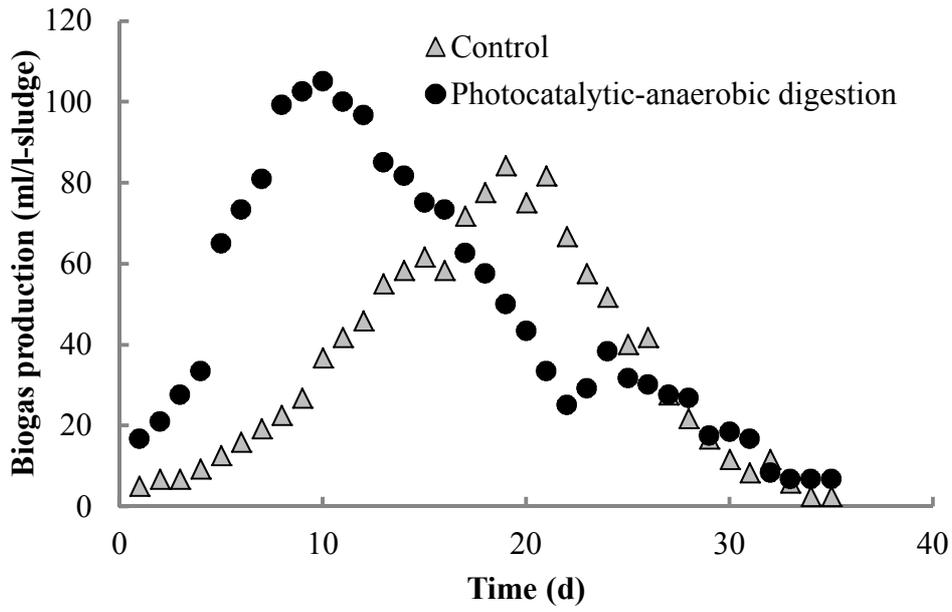
Fig.4.4. Changes of methane yields (a) and concentrations (b) in photocatalytic anaerobic fermenter and control fermenter, respectively.
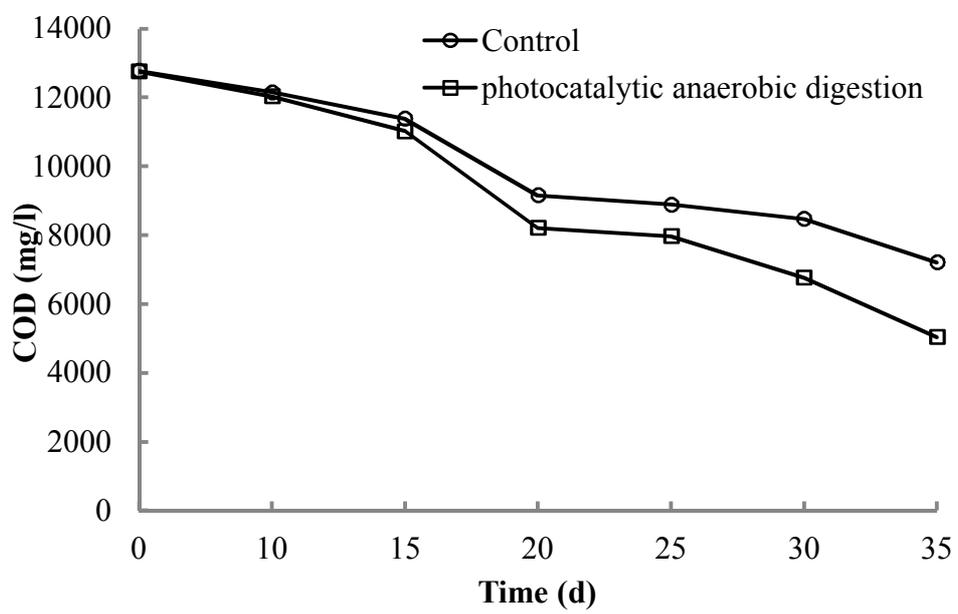
Fig.4.5. COD removal of WAS in the photocatalytic anaerobic fermenter and control

fermenter, respectively.

# Chapter 5 Conclusions and suggestions

In this study, photocatalysis and anaerobic digestion were used to treat waste activated sludge. First, catalyst-suspended photocatalytic reactor was developed to pretreat WAS for enhancing bio-hydrogen production. Then, catalyst-supported photocatalytic reactor with a novel photocatalyst was developed to degrade WAS and simultaneously produce hydrogen by photocatalytic water splitting. Finally, a photocatalytic anaerobic fermenter was developed to degrade WAS and simultaneously produce methane via anaerobic digestion. This fermenter possesses the advantages of photocatalysis and anaerobic digestion and exhibits good performance in methane production and WAS degradation.

## 5.1. Development of $TiO_2$-suspended photocatalytic reactor to treat WAS

From the study, it was investigated into the effect of the reactor design parameters and the operating conditions (such as the shape of trough, circulating speed, $TiO_2$ dosage and initial concentration of WAS) on the photocatalytic degradation of WAS in a sloping trough circulating bed photocatalytic reactor. The following conclusions were obtained.

(1) The STCBPR was effective in degrading WAS. Moreover, it was easy to be operated and maintained.

(2) Nearly 45% of COD and 47% of VS reduction were obtained under 7.5-fold dilution and reaction for 8 h.

(3) Photocatalytic pretreatment increased the SCOD and $NH_4^+$-N concentrations of the WAS.

(4) Photocatalysis pretreated WAS as substrate produced the maximum hydrogen via anaerobic digestion, followed by UV irradiation pretreated WAS. Therefore, the STCBPR could be a better reactor for WAS pretreatment and further enhance the bio-hydrogen production.

## 5.2. Development of $TiO_2$-supported photocatalytic reactor to treat WAS

As a supported catalyst, $TiO_2$ is low efficient for the degradation of WAS. The modification of $TiO_2$ with high photocatalytic activity is necessary. On the basis of this purpose, a modified $TiO_2$ with Ag was developed. The properties and photocatalytic activity of the new photocatalyst were investigated in solar photocatalytic reactor. In order to apply the new photocatalyst, a solar fluidized tubular photocatalytic reactor with a simple light collector was developed. The conclusions were draw as follows:

(1) The photocatalyst of $AgX/TiO_2$ film was synthesized successfully, and its photocatalytic activity was significantly improved due to silver and silver compound ($Ag-Ag_2O-AgCl$) doping on $TiO_2$.

(2) The light collector was simple and effective on enhancing the photocatalytic activity of the photocatalyst.

(3) 69.1% of COD removal and 7866.7 $\mu$mol-$H_2$/L-sludge were achieved in SFTPR

with AgX/TiO$_2$ as photocatalyst for 72 h, which was 50% and 350% higher than in SFTPR with TiO$_2$ as photocatalyst.

## 5. 3. Development of photocatalytic anaerobic fermenter to treat WAS

The catalyst-supported photocatalytic reactor possesses some advantages, such as high degradation efficiency, without separation of catalyst, no inhibition to anaerobic digestion, the photocatalytic anaerobic fermenter with intermittent photocatalytic treatment was developed for WAS degradation and simultaneous biogas production. The conclusions were as follows:

(1) The photocatalytic anaerobic fermenter was effective in degrading WAS. Moreover, it was easy to be operated and maintained.

(2) 60.5% of COD removal and 1266.7 ml-CH$_4$/L-sludge production were obtained during anaerobic digestion process with intermittent photocatalytic treatment. While only 43.5% of COD removal and 932.2 ml-CH$_4$/L-sludge production were obtained in the control fermenter.

(3) Therefore, it is confirmed that intermittent photocatalytic treatment enhanced the WAS degradation and methane production in the anaerobic digestion process of WAS.

## 5.4. Further research

By combination of photocatalysis with anaerobic digestion, a novel photocatalytic

anaerobic fermenter was developed finally for WAS degradation and simultaneously biogas production in batch mode. From the consideration of practical application, continuous experiments at pilot-scale are recommended in the further. The following two points are highly recommended.

(1) A pilot-scale photocatalytic anaerobic fermenter will be set up for the continuous degradation of WAS and simultaneously biogas production. Different organic loading rates and HRT will be tested in the experiments to determine the optimum operating conditions.

(2) The deactivation of photocatalyst during the anaerobic digestion process should be paid attention.

# References

[1] Matsubara M, Itoh T. The present situation and future issues on beneficial use of sewage sludge. Saisei to riyo (Association for Utilization of Sewage Sludge), 2006;29: 19-27 (in Japanese).

[2] Ozaki M, Miyamoto A. Utilization of melt-solidified slag from sewage sludge as construction materials, in The 4th IWA Leading Edge Conference and Exhibition on Water and Wastewater Technologies 2007: Singapore.

[3] Hong J, Otaki M, Jolliet O. Environmental and economic life cycle assessment for sewage sludge treatment processes in Japan. Waste Management 2009;29: 696-703.

[4] Liu X, Liu H, Chen J, Du G, Chen J. Enhancement of solubilization and acidification of waste activated sludge by pretreatment. Waste management 2008;28: 2614-2622.

[5] Feng X, Deng J, Lei H, Bai T, Fan Q, Li Z. Dewaterability of waste activated sludge with ultrasound conditioning. Bioresource Technology 2009; 100:1074-1081.

[6] Tang B, Yu L, Huang S, Luo J, Zhuo Y. Energy efficiency of pretreating excess sewage sludge with microwave irradiation. Bioresource Technology 2010;101:5092-5097.

[7] Citeau M, Olivier J, Mahmoud A, Vaxelaire J, Larue O, Vorobiev E. Pressurised electro-osmotic dewatering of activated and anaerobically digested sludges:

Electrical variables analysis. Water Research 2012;46:4405-4416.

[8] Guan BH, Yu J, Fu HL, Guo MH, Xu XH. Improvement of activated sludge dewaterability by mild thermal treatment in $CaCl_2$ solution. Water Research 2012;46:425-432.

[9] Devlin DC, Esteves SR, Dinsdale RM, Guwy AJ. The effect of acid pretreatment on the anaerobic digestion and dewatering of waste activated sludge. Bioresource Technology 2011;102:4076-4082.

[10] Li H, Jin YY, Mahar RB, Wang ZY, Nie YF. Effects and model of alkaline waste activated sludge treatment. Bioresource Technology 2008;99:5140-5144.

[11] Zitomer DH, Duran M, Albert R, Guven E. Thermophilic aerobic granular biomass for enhanced settleability. Water Research 2007;41:819-825.

[12] Ting CH, Lee DJ. Production of hydrogen and methane from wastewater sludge using anaerobic fermentation. International Journal of Hydrogen Energy 2007;32:677-682.

[13] Paul E, Camacho P, Sperandio M, Ginestet P. Technical and economical evaluation of a thermal, and two oxidative techniques for the reduction of excess sludge production. Process Safety and Environmental Protection 2006;84:247-252.

[14] Wang FY, Rudolph R, Zhu ZH. Sewage sludge technologies. In Sven Erik Jorgensen and Brian Fath (Ed.), Encyclopedia of ecology Oxford, England: Elsevier. 2008.

[15] Mahmood T, Elliott A. A review of secondary sludge reduction technologies for the pulp and paper industry. Water Research 2006;40:2093-112.

[16] Ward AJ, Hobbs PJ, Holliman PJ, Jones DL. Optimisation of the anaerobic digestion of agricultural resources. Bioresource Technology 2008;99:7928-7940.

[17] Kalloum S, Bouabdessalem H, Touzi A, Iddou A, Ouali MS. Biogas production from the sludge of the municipal wastewater treatment plant of Adrar city. Biomass and Bioenergy 2011;35:2554-2560.

[18] Guo L, Li XM, Zeng GM, Zhou Y. Effective hydrogen production using waste sludge and its filtrate. Energy 2010;35:3557-3562

[19] Tanisho S, Kamiya N, Wakao N. Hydrogen evolution of enterobacter aerogenes depending on culture pH: mechanism of hydrogen evolution from NADH by means of membrane-bound hydrogenase. Biochimica et Biophysica Acta (BBA) - Bioenergetics 1989;973:1-6.

[20] Zhang D, Chen Y, Zhao Y, Ye Z. A new process for efficiently producing methane from waste activated sludge: alkaline pretreatment of sludge followed by treatment of fermentation liquid in an EGSB reactor. Environtal Science & Technology 2011;45:803-808.

[21] Yu GH, He PJ, Shao LM, Zhu YS. Extracellular proteins, polysaccharides and enzymes impact on sludge aerobic digestion after ultrasonic pretreatment. Water Research 2008;42:1925-1934.

[22] Yu GH, He PJ, Shao LM, He PP. Stratification structure of sludge flocs with

implications to dewaterability. Environmental Science & Technology 2008; 42:7944-7949.

[23] Gujer W, Zehnder AJB. Conversion processes in anaerobic digestion. Water Science and Technology 1983;15:127-167.

[24] Pilli S, Bhunia P, Yan S, LeBlanc RJ, Tyagi RD, Surampalli RY. Ultrasonic pretreatment of sludge: A review. Ultrasonics Sonochemistry 2011;18:1-18.

[25] Yuan HP, Cheng XB, Chen SP, Zhu NW, Zhou ZY. New sludge pretreatment method to improve dewaterability of waste activated sludge. Bioresource Technology 2011;102:5659-5664.

[26] Mohapatra DP, Brar SK, Tyagi RD, Surampalli RY. Physico-chemical pretreatment and biotransformation of wastewater and wastewater Sludge-Fate of bisphenol A. Chemosphere 2010;78:923-941.

[27] Yu Q, Lei HY, Li Z, Li HL, Chen K, Zhang XH, Liang RL. Physical and chemical properties of waste-activated sludge after microwave treatment. Water Research 2010;44:2841-2849.

[28] Lin Y, Wang D, Wu S, Wang C. Alkali pretreatment enhances biogas production in the anaerobic digestion of pulp and paper sludge. Journal of Hazardous Materials 2009;170:366-373.

[29] Carrere H, Dumas C, Battimelli A, Batstone DJ, Delgenès JP, Steyer JP, Ferrer I. Pretreatment methods to improve sludge anaerobic degradability: A review. Journal of Hazardous Materials 2010;183:1-15.

[30] Saha M, Eskicioglu C, Marin J. Microwave, ultrasonic and chemo-mechanical pretreatments for enhancing methane potential of pulp mill wastewater treatment sludge. Bioresource Technology 2011;102:7815-7826.

[31] Guo L, Li XM, Bo X, Yang Q, Zeng GM, Liao DX, Liu JJ. Impacts of sterilization, microwave and ultrasonication pretreatment on hydrogen producing using waste sludge. Bioresource Technology 2008;99:3651-3658.

[32] Wang H, Wang J, Fang Z, Wang XF, Bu HY. Enhanced bio-hydrogen production by anaerobic fermentation of apple pomace with enzyme hydrolysis. International Journal of Hydrogen Energy 2010;35:8303-8309.

[33] Yang Y, Tsukahara K, Yang R, Zhang Z, Sawayama S. Enhancement on biodegradation and anaerobic digestion efficiency of activated sludge using a dual irradiation process. Bioresource Technology 2011;102:10767-10771.

[34] Agustina TE, Ang HM, Vareek VK. A review of synergistic effect of photocatalysis and ozonation on wastewater treatment. Journal of Photochemistry and Photobiology C: Photochemistry Reviews 2005;6:264-273.

[35] Gaya UI, Abdullah AH. Heterogeneous photocatalytic degradation of organic contaminants over titanium dioxide: A review of fundamentals, progress and problems. Journal of Photochemistry and Photobiology C: Photochemistry Reviews 2008;9:1-12.

[36] Almquist CB, Biswas P. A mechanistic approach to modeling the effect of dissolved oxygen in photo-oxidation reactions on titanium dioxide in aqueous

systems, Chemical Engineering Science 2001;56:3421–3430.

[37] Silvestre CIC, Frigerio C, Santos JLM, Lima JLFC. Quantum dots assisted photocatalysis for the chemiluminometric determination of chemical oxygen demand using a single interface flow system. Analytica chimica acta 2011;699:193-197.

[38] Chong MN, Jin B, Chow CWK, Saint C. Recent developments in photocatalytic water treatment technology: A review. Water Research 2010;44:2997-3027.

[39] Badawy MI, Ghaly MY, Ali MEM. Photocatalytic hydrogen production over nanostructured mesoporous titania from olive mill wastewater. Desalination 2011;267:250-255.

[40] Noorjahan M, Reddy MP, Kumari VD, Lavédrine B, Boule P, Subrahmanyam M. Photocatalytic degradation of H-acid over a novel $TiO_2$ thin film fixed bed reactor and in aqueous suspensions. Journal of Photochemistry and Photobiology A: Chemistry 2003;156:179-187.

[41] Jiang H, Zhang G, Huang T, Chen J, Wang Q, Meng Q. Photocatalytic membrane reactor for degradation of acid red B wastewater. Chemical Engineering Journal 2010;156:571-577.

[42] Subramanian M, Kannan A. Photocatalytic degradation of phenol in a rotating annular reactor. Chemical Engineering Science 2010;65:2727-2740.

[43] Huelgas A, Funamizu N. Flat-plate submerged membrane bioreactor for the treatment of higher-load graywater. Desalination 2010;250:162-166.

[44] Zayani G, Bousselmi L, Mhenni F, Ghrabi A. Solar photocatalytic degradation of commercial textile azo dyes: Performance of pilot plant scale thin film fixed-bed reactor. Desalination 2009;246:344-352.

[45] Sylwia M. Photocatalytic membrane reactors (PMRs) in water and wastewater treatment. A review. Separation and Purification Technology 2010;73:71-91.

[46] Flakker CL, Muggli DS. Factors affecting methanol photocatalytic oxidation and catalyst attrition in a fluidized-bed reactor. Applied Catalysis B: Environmental 2008;84:706-714.

[47] Denny F, Scott J, Pareek V, Peng GD, Amal R. CFD modelling for a $TiO_2$-coated glass-bead photoreactor irradiated by optical fibres: Photocatalytic degradation of oxalic acid. Chemical Engineering Science 2009;64:1695-1706.

[48] Boyjoo Y, Ang M, Pareek V. Light intensity distribution in multi-Lamp photocatalytic reactors. Chemical Engineering Science 2013;93:11-21.

[49] McCullagh C, Skillen N, Adams M, Robertson PKJ. Photocatalytic reactors for environmental remediation: A review. Journal of Chemical Technology & Biotechnology 2011;86:1002-1017.

[50] Chiou CH, Wu CY, Juang RS. Influence of operating parameters on photocatalytic degradation of phenol in $UV/TiO_2$ process. Chemical Engineering Journal 2008;139:322-329.

[51] Merabet S, Bouzaza A, Wolbert D. Photocatalytic degradation of indole in a circulating upflow reactor by $UV/TiO_2$ process-influence of some operating

parameters. Journal of Hazardous Materials 2009;166:1244-1249.

[52] Sun JH, Wang XL, Sun JY, Sun RX, Sun SP, Qiao LP. Photocatalytic degradation and kinetics of Orange G using nano-sized $Sn(IV)/TiO_2/AC$ photocatalyst. Journal of Molecular Catalysis A: Chemical 2006;260:241-246.

[53] Akpan UG, Hameed BH. Parameters affecting the photocatalytic degradation of dyes using $TiO_2$-based photocatalysts: a review. Journal of Hazardous Materials 2009;170:520-529.

[54] Lin Y, Ferronato C, Deng N, Chovelon JM. Study of benzylparaben photocatalytic degradation by $TiO_2$. Applied Catalysis B: Environmental 2011;104:353-360.

[55] Mohammadi MR, Cordero-Cabrera MC, Fray DJ, Ghorbani M. Preparation of high surface area titania ($TiO_2$) films and powders using particulate sol–gel route aided by polymeric fugitive agents. Sensors and Actuators B: Chemical 2006;120:86-95.

[56] Jia C, Wang Y, Zhang C, Qin Q. $UV$-$TiO_2$ photocatalytic degradation of landfill leachate. Water, Air, & Soil Pollution 2010;217:375-385.

[57] Chong MN, Jin B, Chow CWK, Saint C. Recent developments in photocatalytic water treatment technology: A review. Water Research 2010;44:2997-3027.

[58] Malagutti AR, Mourao HAJL, Garbin JR, Ribeiro C. Deposition of $TiO_2$ and $Ag:TiO_2$ thin films by the polymeric precursor method and their application in the photodegradation of textile dyes. Applied Catalysis B: Environmental

2009;90:205-212.

[59] Krejčíková S, Matějová L, Kočí K, Obalová L. Preparation and characterization of Ag-doped crystalline titania for photocatalysis applications. Applied Catalysis B: Environmental, 2012. 111-112: 119-125.

[60] Ahmed S, Rasul MG, Martens WN, Brown R, Hashib M.A. Heterogeneous photocatalytic degradation of phenols in wastewater: A review on current status and developments. Desalination 2010;261:3-18.

[61] Zhao Y, Yang B, Xu J, Fu Z, Wu M, Li F. Facile synthesis of Ag nanoparticles supported on $TiO_2$ inverse opal with enhanced visible-light photocatalytic activity. Thin Solid Films 2012;520:3515-3522.

[62] Melián EP, Díaz OG, Rodríguez, Doña JM, Colón G, Navío JA, Macías M, Peña JP. Effect of deposition of silver on structural characteristics and photoactivity of $TiO_2$-based photocatalysts. Applied Catalysis B: Environmental 2012; 127:112-120.

[63] Choi M, Shin KH, Jang J. Plasmonic photocatalytic system using silver chloride/silver nanostructures under visible light. Journal of Colloid and Interface Science 2010;341:83-87.

[64] Li Q, Chen L, Lu G. Visible-Light-Induced photocatalytic hydrogen generation on dye-sensitized multiwalled carbon nanotube Pt catalyst. The Journal of Physical Chemistry C 2007;111:11494-11499.

[65] Ma B, Guo J, Dai WL, Fan K. Ag-AgCl/$WO_3$ hollow sphere with flower-like

structure and superior visible photocatalytic activity. Applied Catalysis B: Environmental 2012;123:193-199.

[66] Fernández-Ibáñez P, Sichel C, Polo-Lópe MI, de Cara-García M, Tello JC. Photocatalytic disinfection of natural well water contaminated by Fusarium solani using $TiO_2$ slurry in solar CPC photo-reactors. Catalysis Today 2009;144:62-68.

[67] Jing D, Liu H, Zhang X, Zhao L, Guo L. Photocatalytic hydrogen production under direct solar light in a CPC based solar reactor: Reactor design and preliminary results. Energy Conversion and Management 2009;50:2919-2926.

[68] Rao NN, Chaturvedi V, Puma GL. Novel pebble bed photocatalytic reactor for solar treatment of textile wastewater. Chemical Engineering Journal 2012; 184:90-97.

[69] Augugliaro V, Bellardita M, Loddo V, Palmisano G, Palmisano L, Yurdakal S. Overview on oxidation mechanisms of organic compounds by $TiO_2$ in heterogeneous photocatalysis. Journal of Photochemistry and Photobiology C: Photochemistry Reviews 2012;13:224-245.

[70] Kyung H, Lee J, Choi W. Simultaneous and synergistic conversion of dyes and heavy metal Ions in aqueous $TiO_2$ suspensions under visible-light illumination. Environmental Science & Technology 2005;39:2376-2382.

[71] Marugán J, Grieken RV, Pablos C, Satuf ML, Cassano AE, Alfano OM. Rigorous kinetic modelling with explicit radiation absorption effects of the photocatalytic inactivation of bacteria in water using suspended titanium dioxide. Applied

Catalysis B: Environmental 2011;102:404-416.

[72] Fotiadis C, Xekoukoulotakis N, Mantzavinos D. Photocatalytic treatment of wastewater from cottonseed processing: Effect of operating conditions, aerobic biodegradability and ecotoxicity. Catalysis Today 2007;124:247-253.

[73] Kim MJ, Yang YN, Morikawa-Sakura MS, Wang QH, Lee MV, Lee DY, Feng CP, Zhang ZY. Hydrogen production by anaerobic co-digestion of rice straw and sewage sludge. International Journal of Hydrogen Energy 2012;37:3142-3149.

[74] Eaton AD, American PHA, American WWA, Water EF. Standard methods for the examination of water and wastewater. 21st ed. Washington, DC. 2005.

[75] Khongnakorn W, Wisniewski C, Pottier L, Vachoud L. Physical properties of activated sludge in a submerged membrane bioreactor and relation with membrane fouling. Separation and Purification Technology 2007;55:125-131.

[76] Yang F, Bick A, Shandalov S, Brenner A, Oron G. Yield stress and rheological characteristics of activated sludge in an airlift membrane bioreactor. Journal of Membrane Science 2009;334:83-90.

[77] Hasar H, Kinaci C, Ünlü A, Toğrul H, Ipek U. Rheological properties of activated sludge in a sMBR. Biochemical Engineering Journal 2004;20:1-6.

[78] Merabet S, Bouzaza A, Wolbert D. Photocatalytic degradation of indole in a circulating upflow reactor by UV/TiO$_2$ process-Influence of some operating parameters. Journal of Hazardous Materials 2009;166:1244-1249.

[79] Ballari MdlM, Alfano OM, Cassano AE. Mass transfer limitations in slurry

photocatalytic reactors: Experimental validation. Chemical Engineering Science 2010;65:4931-4942.

[80] Sarasidis VC, Patsios SI, Karabelas AJ. A hybrid photocatalysis-ultrafiltration continuous process: The case of polysaccharide degradation. Separation and Purification Technology 2011;80:73-80.

[81] Tokumura M, Katoh H, Katoh T, Znad HT, Kawase Y. Solubilization of excess sludge in activated sludge process using the solar photo-Fenton reaction. Journal of Hazardous Materials 2009;162:1390-1396.

[82] Yan S, Miyanaga K, Xing XH, Tanji Y. Succession of bacterial community and enzymatic activities of activated sludge by heat-treatment for reduction of excess sludge. Biochemical Engineering Journal 2008;39:598-603.

[83] Braguglia CM, Gianico A, Mininni G. Laboratory-scale ultrasound pretreated digestion of sludge: Heat and energy balance. Bioresource Technology 2011;102:7567-7573.

[84] Chang CJ, Tyagi VK, Lo SL. Effects of microwave and alkali induced pretreatment on sludge solubilization and subsequent aerobic digestion. Bioresource Technology 2011;102:7633-7640.

[85] Chen K, Lei H, Li Y, Li H, Zhang X, Yao C. Physical and chemical characteristics of waste activated sludge treated with electric field. Process Safety and Environmental Protection 2011;89:327-333.

[86] Apul OG, Sanin FD. Ultrasonic pretreatment and subsequent anaerobic digestion

under different operational conditions. Bioresource Technology 2010; 101:8984-8992.

[87] Feng X, Lei H, Deng J, Yu Q, Li H. Physical and chemical characteristics of waste activated sludge treated ultrasonically. Chemical Engineering and Processing: Process Intensification 2009;48:187-194.

[88] Miranda-García N, Suárez S, Sánchez B, Coronado JM, Malato S, Ignacio Maldonado M. Photocatalytic degradation of emerging contaminants in municipal wastewater treatment plant effluents using immobilized $TiO_2$ in a solar pilot plant. Applied Catalysis B: Environmental 2011;103:294-301.

[89] Guo L, Li XM, Bo X, Yang Q, Zeng GM, Liao D, Liu JJ. Impacts of sterilization, microwave and ultrasonication pretreatment on hydrogen producing using waste sludge. Bioresource Technology 2008;99:3651-3658.

[90] Pulido Melián E, González Díaz O, Doña Rodríguez JM, Colón G, Navío JA, Macías M, Pérez Peña J. Effect of deposition of silver on structural characteristics and photoactivity of $TiO_2$-based photocatalysts. Applied Catalysis B: Environmental 2012;127:112-120.

[91] Wang Q, Yang X, Liu D, Zhao J. Fabrication, characterization and photocatalytic properties of Ag nanoparticles modified $TiO_2$ NTs. Journal of Alloys and Compounds 2012;527:106-111.

[92] van Grieken R, Marugan J, Sordo C, Martinez P, Pablos C. Photocatalytic inactivation of bacteria in water using suspended and immobilized silver-$TiO_2$.

Applied Catalysis B: Environmental 2009;93:112-118.

[93] Rosseler O, Shankar MV, Du MK, Schmidlin L, Keller N, Keller V. Solar light photocatalytic hydrogen production from water over Pt and Au/TiO$_2$ (anatase/rutile) photocatalysts: Influence of noble metal and porogen promotion. Journal of Catalysis 2010;269:179-190.

[94] Yu J, Qi L, Jaroniec M. Hydrogen production by photocatalytic water splitting over Pt/TiO$_2$ nanosheets with exposed (001) facets. Journal of Physical Chemistry C 2010;114:13118-13125.

[95] Thungklin P, Reungsang A, Sittijunda S. Hydrogen production from sludge of poultry slaughterhouse wastewater treatment plant pretreated with microwave. International Journal of Hydrogen Energy 2011;36:8751-8757.

[96] Lee J, Kim J, Choi W. TiO$_2$ Photocatalysis for the redox conversion of aquatic pollutants. American Chemical Society 2011;1071:199-222. In Aquatic Redox Chemistry; Tratnyek P; American Chemical Society: Washington, DC, 2011.

[97] da Rocha OR, Dantas RF, Duarte MM, Duarte MM, da Silva VL. Oil sludge treatment by photocatalysis applying black and white light. Chemical Engineering Journal 2010;157:80-85.

[98] Laurent J, Casellas M, Carrère H, Dagot C. Effects of thermal hydrolysis on activated sludge solubilization, surface properties and heavy metals biosorption. Chemical Engineering Journal 2011;166:841-849.

[99] Khamtib S, Plangklang P, Reungsang A. Optimization of fermentative hydrogen

production from hydrolysate of microwave assisted sulfuric acid pretreated oil palm trunk by hot spring enriched culture. International Journal of Hydrogen Energy 2011;36:14204-14216.

[100] Wilson CA, Novak JT. Hydrolysis of macromolecular components of primary and secondary wastewater sludge by thermal hydrolytic pretreatment. Water Research 2009;43:4489-4498.

[101] Yang Q, Luo K, Li XM, Wang DB, Zheng W, Zeng GM, Liu JJ. Enhanced efficiency of biological excess sludge hydrolysis under anaerobic digestion by additional enzymes. Bioresource Technology 2010;101:2924-2930.

[102] Chen D, Ray AK. Removal of toxic metal ions from wastewater by semiconductor photocatalysis. Chemical Engineering Science 2001; 56:1561-1570.

[103] Boroski M, Rodrigues AC, Garcia JC, Gerola A, Nozaki J, Hioka N. The effect of operational parameters on electro-coagulation-flotation process followed by photocatalysis applied to the decontamination of water effluents from cellulose and paper factories. Journal of Hazardous Materials 2008;160(1):135-41.

[104] Jamil TS, Ghaly MY, El-Seesy IE, Souaya ER, Nasr RA. A comparative study among different photochemical oxidation processes to enhance the biodegradability of paper mill wastewater. Journal of Hazardous Materials 2011;185:353-358.

[105] Chu CP, Lee DJ, Chang BV, You CH, Liao CS, Tay JH. Anaerobic digestion of

polyelectrolyte flocculated waste activated sludge. Chemosphere 2003; 53:757-764.

[106] Chu L, Wang J, Wang B, Xing XH, Yan S, Sun X, Jurcik B. Changes in biomass activity and characteristics of activated sludge exposed to low ozone dose. Chemosphere 2009;77:269-72.

[107] Fan W, Lai Q, Zhang Q, Wang Y. Nanocomposites of $TiO_2$ and reduced graphene oxide as efficient photocatalysts for hydrogen evolution. The Journal of Physical Chemistry C 2011;115:10694-10701.

# Acknowledgements

Finally, I would like to thank my parents and my wife Huiling Zhang. This dissertation would not have been completed without their love and support.

# Appendix

[1] **Chunguang Liu**, Yingnan Yang, Qinghong Wang, Mijung Kim, Qingrong Zhu, Dawei Li, Zhenya Zhang. Photocatalytic degradation of waste activated sludge using a circulating bed photocatalytic reactor for improving biohydrogen production. Bioresource Technology 2012;125:30-36.

[2] **Chunguang Liu**, Wansheng Shi, Mijung Kim, Yingnan Yang, Zhongfang Lei, Zhenya Zhang. Photocatalytic pretreatment for the redox conversion of waste activated sludge to enhance biohydrogen production. International Journal of Hydrogen Energy 2013;38:7246-7252.

[3] **Chunguang Liu**, Zhongfang Lei, Yingnan Yang, Haifeng Wang, Zhenya Zhang. Improvement in settleability and dewaterability of waste activated sludge by solar photocatalytic treatment in Ag/TiO$_2$-coated glass tubular reactor. Bioresource Technology 2013;137:57-62.

[4] **Chunguang Liu**, Zhongfang Lei, Yingnan Yang, Zhenya Zhang. Preliminary trial on degradation of waste activated sludge and simultaneous hydrogen production in a newly-developed solar photocatalytic reactor with AgX/TiO$_2$-coated glass tubes. Water Research 2013;47:4986-4992.

[5] Wansheng Shi, **Chunguang Liu**, Dahu Ding, Zhongfang Lei, Yingnan Yang, Chuanping Feng, Zhenya Zhang. Immobilization of heavy metals in sewage sludge by using subcritical water technology. Bioresource Technology 2013;137:18-24.

[6] Mijung Kim, **Chunguang Liu**, Jin-Won Noh, Yingnan Yang, Sechang Oh, Kazuya Shimizu, Dong-Yeol Lee, Zhenya Zhang. Hydrogen and methane production from untreated rice straw and raw sewage sludge under thermophilic anaerobic conditions. International Journal of Hydrogen Energy 2013;38:8648-8656.

[7] Mijung Kim, **Chunguang Liu**, Sechang Oh, Randeep Rakwal and Zhenya Zhang. Biohydrogen production from sterilized sewage sludge as a substrate using mixed cultures. IPCBEE vol.51 (2013), DOI: 10.7763/IPCBEE. 2013. V51. 17

[8] Mijung Kim, Sechang Oh, Randeep Rakwal, **Chunguang Liu**, Zhenya Zhang, Simultaneous organic solids disintegration and fermentative hydrogen production by pretreated sludge generated from wastewater treatment plant. International Journal of Environmental Science and Development (2013), DOI:10.7763/IJESD

[9] Wansheng Shi, **Chunguang Liu**, Youju Shu, Chuanping Feng, Zhongfang Lei, Zhenya Zhang. Synergistic effect of rice husk addition on hydrothermal treatment of sewage sludge: Fate and environmental risk of heavy metals. Bioresource Technology (2013), DOI: http://dx.doi.org/10.1016/j.biortech.2013.09.114.